

Analog Circuit Design Laboratory

Lab Report

written by:

Lorenz Buchinger

Agustín Sevil de Llobet

Power Electronics Engineering

FH JOANNEUM – University of Applied Sciences, Austria

Graz, January 1, 1991

Contents

| | |
|---|----------|
| 1 Computer Lab | 1 |
| 1.1 Noise Analysis with PSpice | 1 |
| 1.1.1 Task Description | 1 |
| 1.1.2 Schematic | 1 |
| 1.1.3 Curves & Diagrams | 3 |
| 1.1.4 Discussion of Measurement Results | 4 |
| 2 Electronic Lab | 6 |
| 2.1 Active Band-pass Filter | 6 |
| 2.1.1 Task Description | 6 |
| 2.1.2 Schematic | 6 |
| 2.1.3 Formulas and Calculations | 7 |
| 2.1.4 Table(s) with Measurement Results | 7 |
| 2.1.5 Curves & Diagrams | 9 |
| 2.1.6 Discussion of Measurement Results | 14 |
| 2.2 ADC-Driver And Anti-aliasing Filter | 15 |
| 2.2.1 Task Description | 15 |
| 2.2.2 Schematic | 16 |
| 2.2.3 Formulas and Calculations | 16 |
| 2.2.4 Table(s) with Measurement Results | 20 |
| 2.2.5 Curves & Diagrams | 21 |
| 2.2.6 Discussion of Measurement Results | 24 |
| 2.3 Switched Capacitor Filter | 25 |
| 2.3.1 Task Description | 25 |
| 2.3.2 Schematic | 25 |

| | | |
|----------|---|-----------|
| 2.3.3 | Formulas and Calculations | 26 |
| 2.3.4 | Table(s) with Measurement Results | 26 |
| 2.3.5 | Curves & Diagrams | 28 |
| 2.3.6 | Discussion of Measurement Results | 30 |
| E | Equipment Used | 31 |
| A | Appendix | 32 |
| A.1 | Calculations | 33 |
| | A.1.1 Active Band-pass Filter | 33 |
| A.2 | Matlab | 36 |
| A.3 | Measurements | 36 |

1

Computer Lab

1.1 Noise Analysis with PSpice

1.1.1 Task Description

The task of this lab session was to conduct simulations of transistor and OpAmp circuits in PSpice, and to analyze the noise generated by the different components of the circuits. The circuits that were simulated include a single stage emitter circuit, an inverting amplifier, and a non-inverting amplifier. The noise spectral voltage density of the output of each circuit was analyzed, and the contribution of each individual resistor to the overall noise was also examined.

1.1.2 Schematic

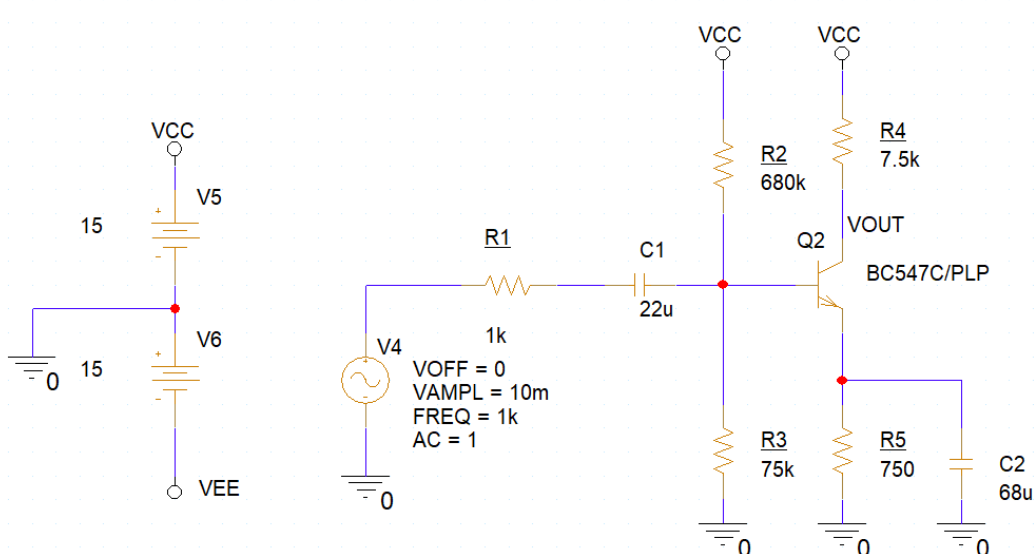


Figure 1.1: Schematic of the single stage emitter circuit used for simulation.

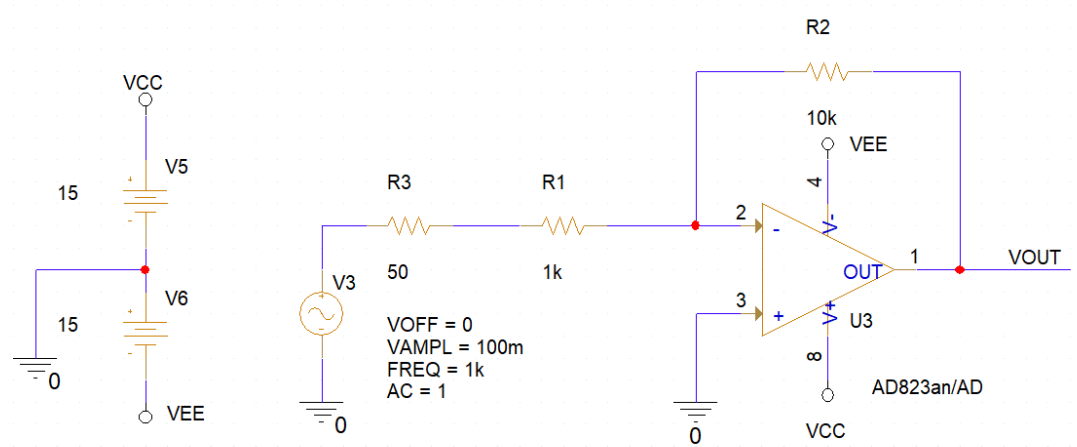


Figure 1.2: Schematic of the inverting amplifier circuit used for simulation.

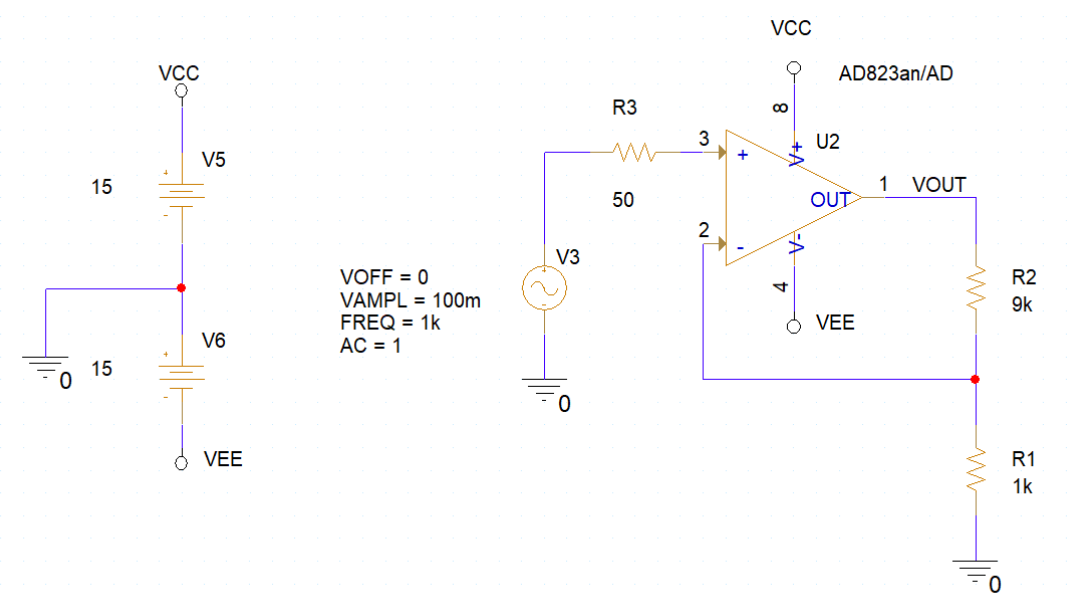


Figure 1.3: Schematic of the non-inverting amplifier circuit used for simulation.

1.1.3 Curves & Diagrams

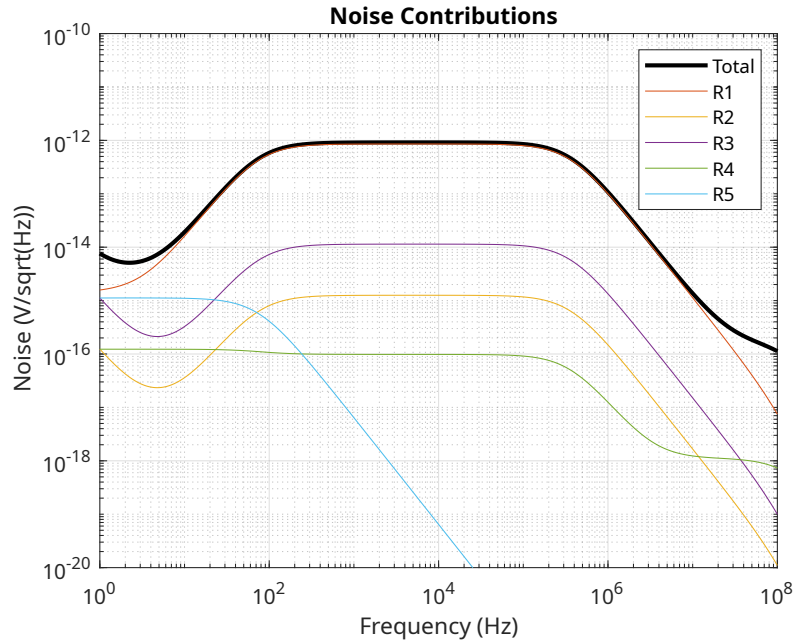


Figure 1.4: Noise spectral voltage density of the single stage emitter circuits output. The simulation results of the noise generated by each individual resistor is also depicted.

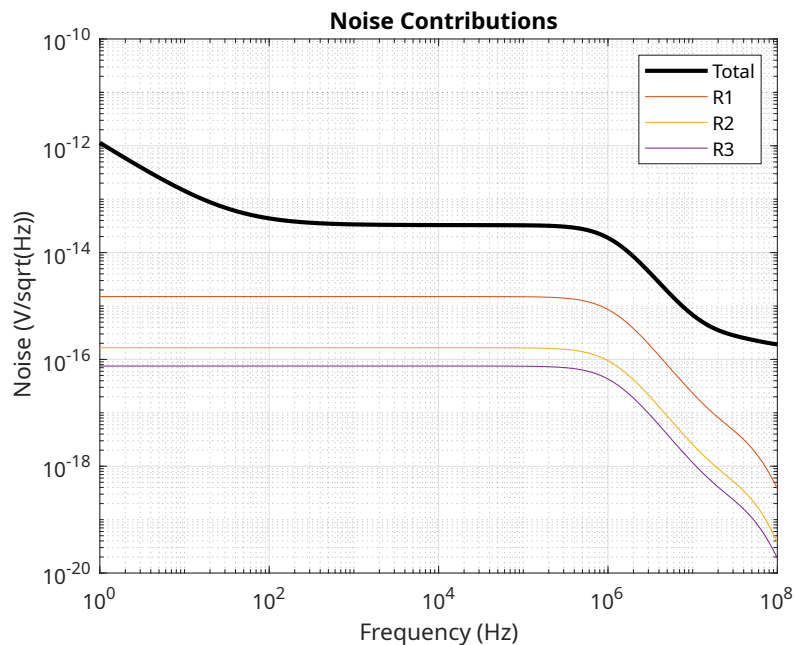


Figure 1.5: Noise spectral voltage density of the inverting amplifiers output. The simulation results of the noise generated by each individual resistor is also depicted.

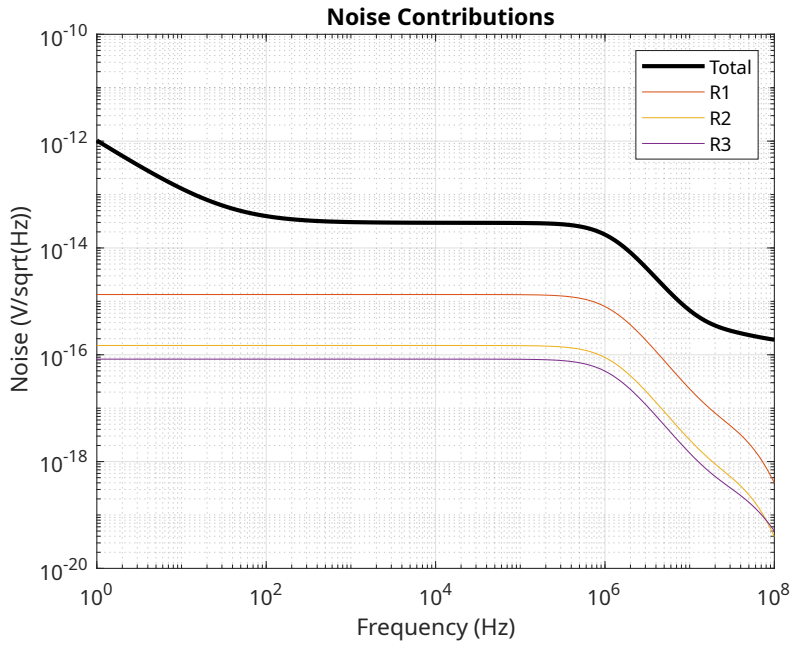


Figure 1.6: Noise spectral voltage density of the non-inverting amplifiers output. The simulation results of the noise generated by each individual resistor is also depicted.

1.1.4 Discussion of Measurement Results

The measured noise spectral voltage density of the emitter follower stage (figure 1.4) shows a similar trend as the emitter followers magnitude response. The emitter follower effectively acts as a bandpass-filter with a very wide pass band. The lower corner frequency of the pass band is determined by the value of the input coupling capacitor and the upper corner frequency by the transistors parasitic capacitances. The thermal noise originating from the resistors is amplified according to the passband characteristics of the emitter follower. R4 and R5 are exceptions because they are not affected by the input coupling capacitor and therefore have no lower corner frequency. R1 is the biggest contributor to the thermal noise even though it has a relatively low resistance because its noise acts as an input signal to the amplifier and is therefore amplified by the gain of the emitter follower.

The shot noise, caused by the transistor, is also visible at lower frequencies. It can be seen when looking at the noise of R3, R4 and the total output noise.

The inverting and non-inverting amplifier stages show an almost identical noise spectral voltage density (figures 1.5 and 1.6). The same behavior observed in the emitter follower where the noise spectral density behaves similar to the magnitude response of the amplifier can also be seen in these two OpAmp amplifier stages. The low-pass filter behavior of the amplifiers can be observed in the

noise spectrum. The OpAmps shot noise is also visible at lower frequencies and can only evident in the total noise and is not present in the individual resistors noise curves because the shot noise is generated by the OpAmp itself and not by the resistors.

2

Electronic Lab

2.1 Active Band-pass Filter

2.1.1 Task Description

A second-order active bandpass filter was designed using the LM4562 dual operational amplifier by cascading two staggered tuned first-order bandpass stages in multi-feedback topology. The transfer function and component values were calculated manually according to the given specifications (Butterworth and 1 dB Chebyshev, 4–5 kHz, 20 dB gain). E24-series components with 1% tolerance were chosen.

The circuit was simulated in PSpice (transient, AC, noise and Monte Carlo analysis), implemented on a prototype board with ± 5 V supply, and experimentally characterized. Frequency response, passband gain, 3 dB corner frequencies and step response were measured and compared with simulation results in a combined Bode plot.

Finally, the output noise behavior was analyzed and discussed in the report.

2.1.2 Schematic

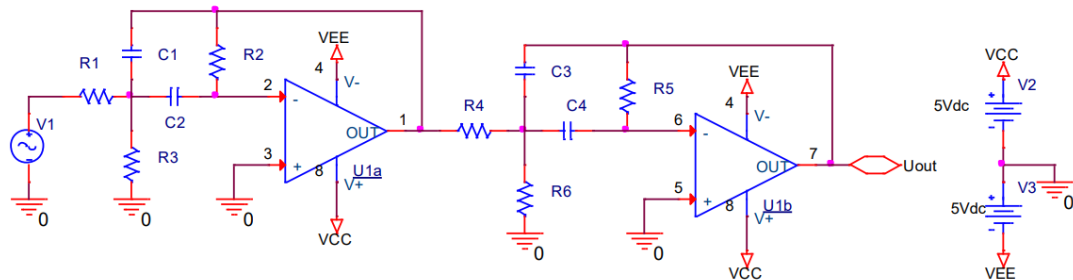


Figure 2.1: Schematic of the second order band pass filter.

2.1.3 Formulas and Calculations

The calculations were done by hand. A scan of the hand written notes can be found in section A.1.1 of the appendix

2.1.4 Table(s) with Measurement Results

Table 2.1: Component values for Butterworth band-pass filter

| | Calculated | Chosen | Measured |
|---------------------------|------------|--------|----------|
| R_1 in $\text{k}\Omega$ | 5.448 | 5.6 | 5.5831 |
| R_2 in $\text{k}\Omega$ | 48.880 | 47 | 46.943 |
| R_3 in Ω | 303.59 | 300 | 298.59 |
| R_4 in $\text{k}\Omega$ | 4.650 | 4.7 | 4.6045 |
| R_5 in $\text{k}\Omega$ | 41.718 | 43 | 42.798 |
| R_6 in Ω | 259.11 | 270 | 269.01 |
| C_1 in nF | - | 10 | 10.03 |
| C_2 in nF | - | 10 | 10.09 |
| C_3 in nF | - | 10 | 10.03 |
| C_4 in nF | - | 10 | 10.10 |

Table 2.2: Component values for Chebyshev 1 dB band-pass filter

| | Calculated | Chosen | Measured |
|--------------------|------------|--------|----------|
| R_1 in $k\Omega$ | 7.532 | 7.5 | - |
| R_2 in $k\Omega$ | 124.641 | 120 | - |
| R_3 in Ω | 117.89 | 120 | - |
| R_4 in $k\Omega$ | 6.492 | 6.2 | - |
| R_5 in $k\Omega$ | 107.432 | 110 | - |
| R_6 in Ω | 101.613 | 100 | - |
| C_1 in nF | - | 10 | 10.03 |
| C_2 in nF | - | 10 | 10.09 |
| C_3 in nF | - | 10 | 10.03 |
| C_4 in nF | - | 10 | 10.10 |

The measured resistor values show deviations below 1% with respect to the nominal chosen E24 values, which confirms the specified tolerance class. The capacitor measurements also confirm the 1% NP0 specification and therefore only introduce minor shifts in the center frequency.

Table 2.3: Center and corner frequencies with their corresponding gain values.

| | -3dB Corner Frequency | Center Frequency | +3dB Corner Frequency |
|-----------------|-----------------------|------------------|-----------------------|
| Frequency in Hz | 4.32 | 4.57 | 4.94 |
| Gain in dB | 19.3 | 22.3 | 19.3 |

The measurements for the bode plot can be found at the appendix in table A.1.

2.1.5 Curves & Diagrams

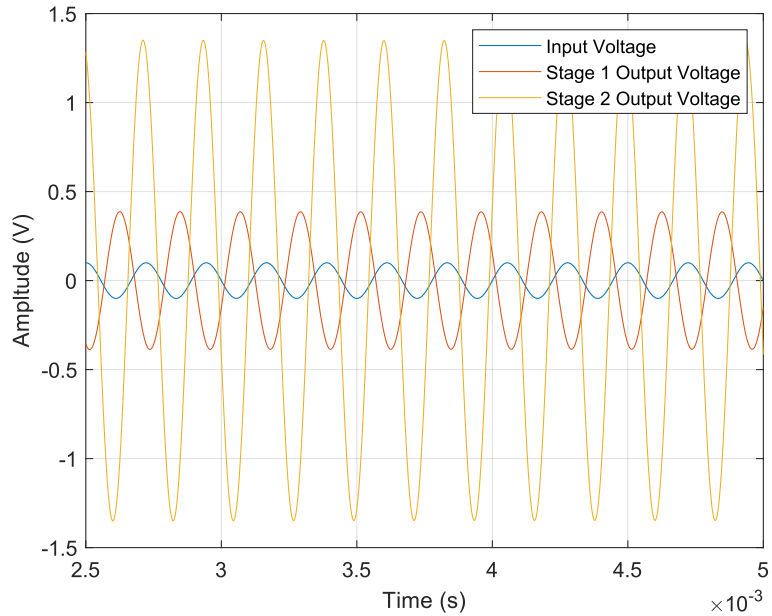


Figure 2.2: Transient simulation showing the sinusoidal input voltage and the output voltage of each of the two amplifier stages.

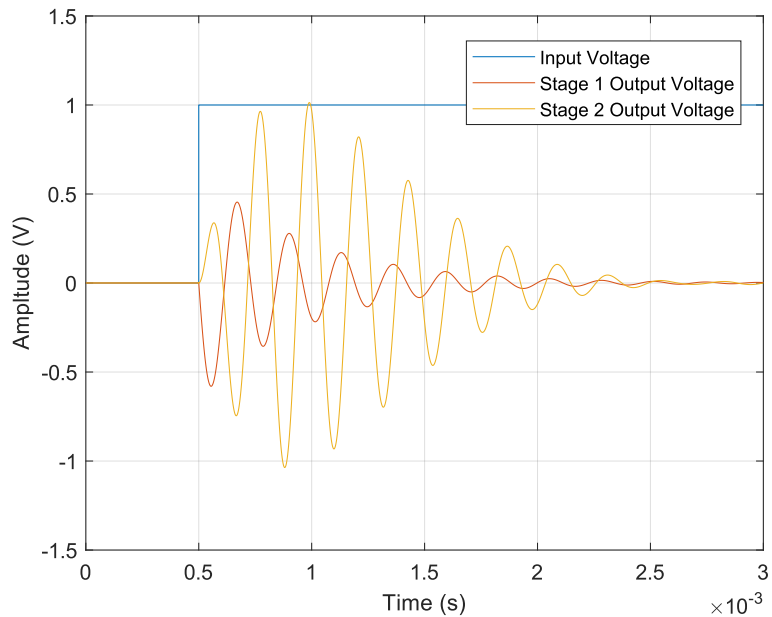


Figure 2.3: Transient simulation showing the step response of both amplifier stages after applying a signal transitioning from 0 V to 1 V to the input.

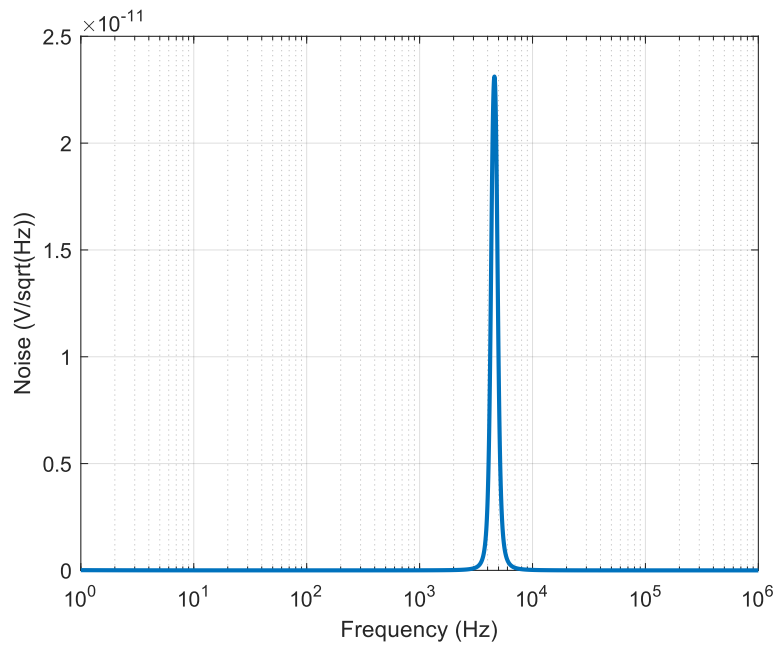


Figure 2.4: Simulation results of the noise spectral voltage density.

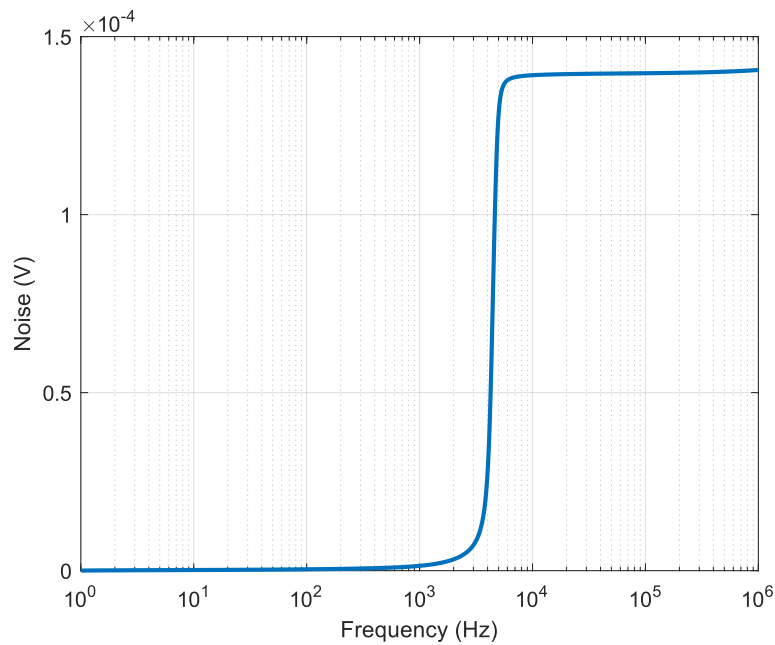


Figure 2.5: Simulation results of the total output noise voltage.

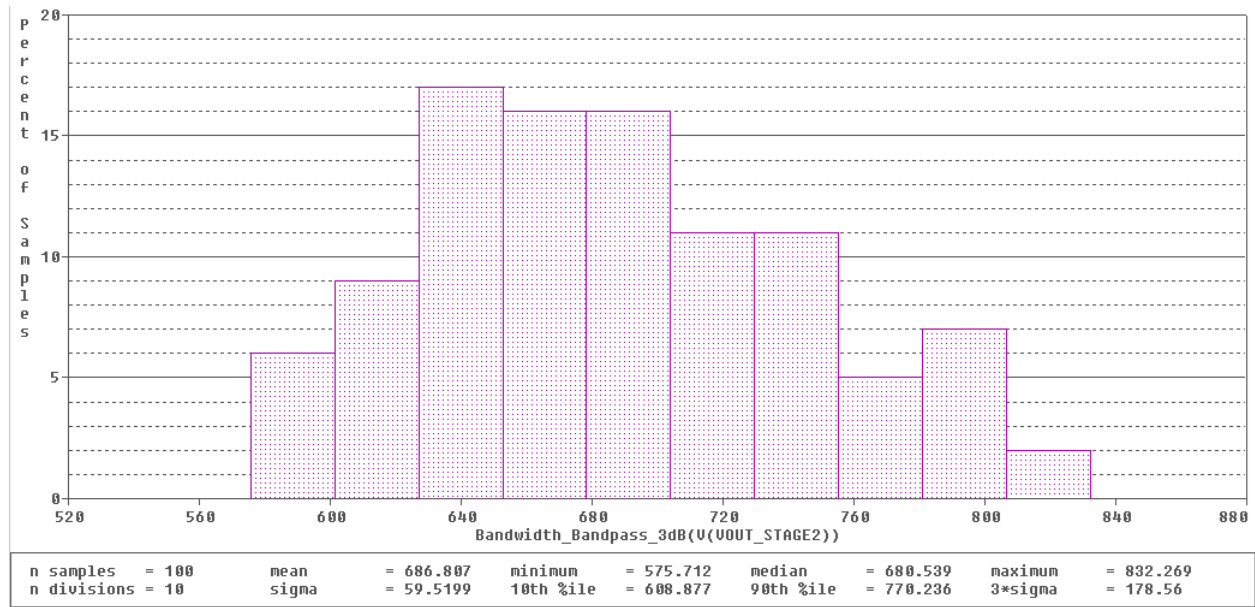


Figure 2.6: Monte Carlo simulation of the 3 db bandwidth. 1% tolerances were used for both resistors and capacitors.

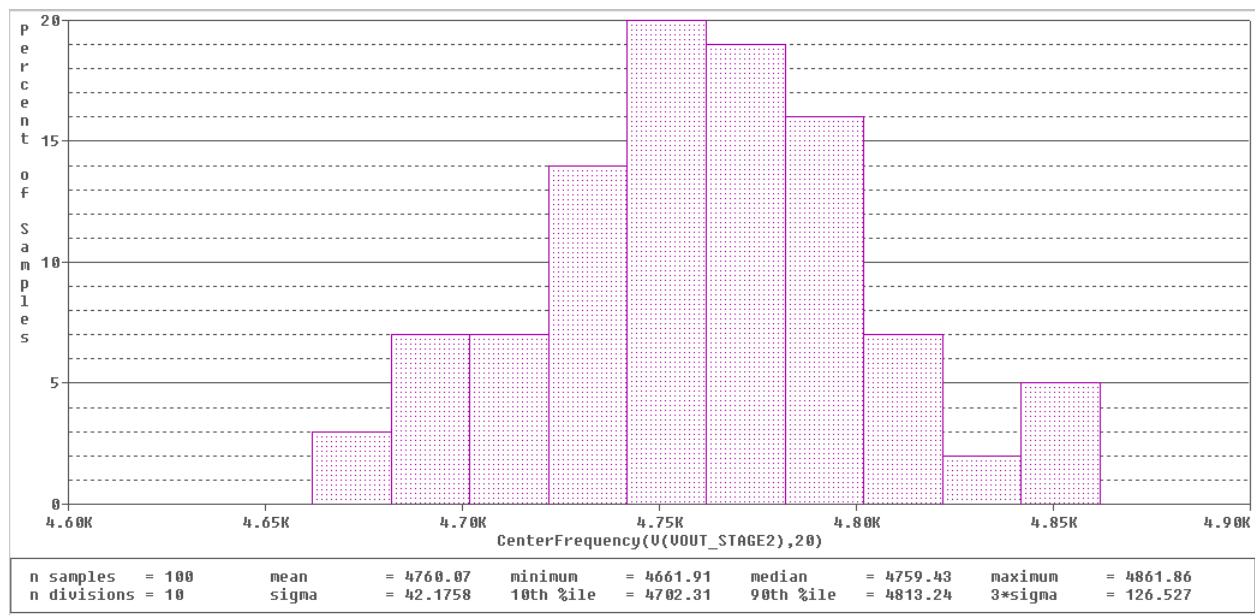


Figure 2.7: Monte Carlo simulation of the center frequency. 1% tolerances were used for both resistors and capacitors.

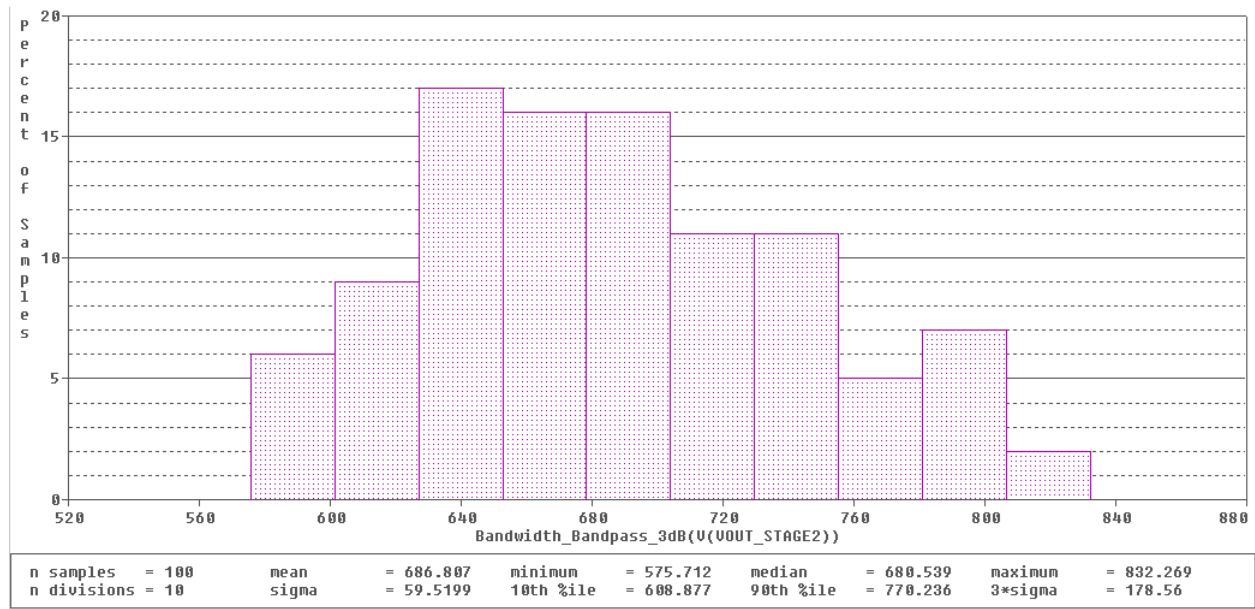


Figure 2.8: Monte Carlo simulation of the gain variation. 1% tolerances were used for both resistors and capacitors.

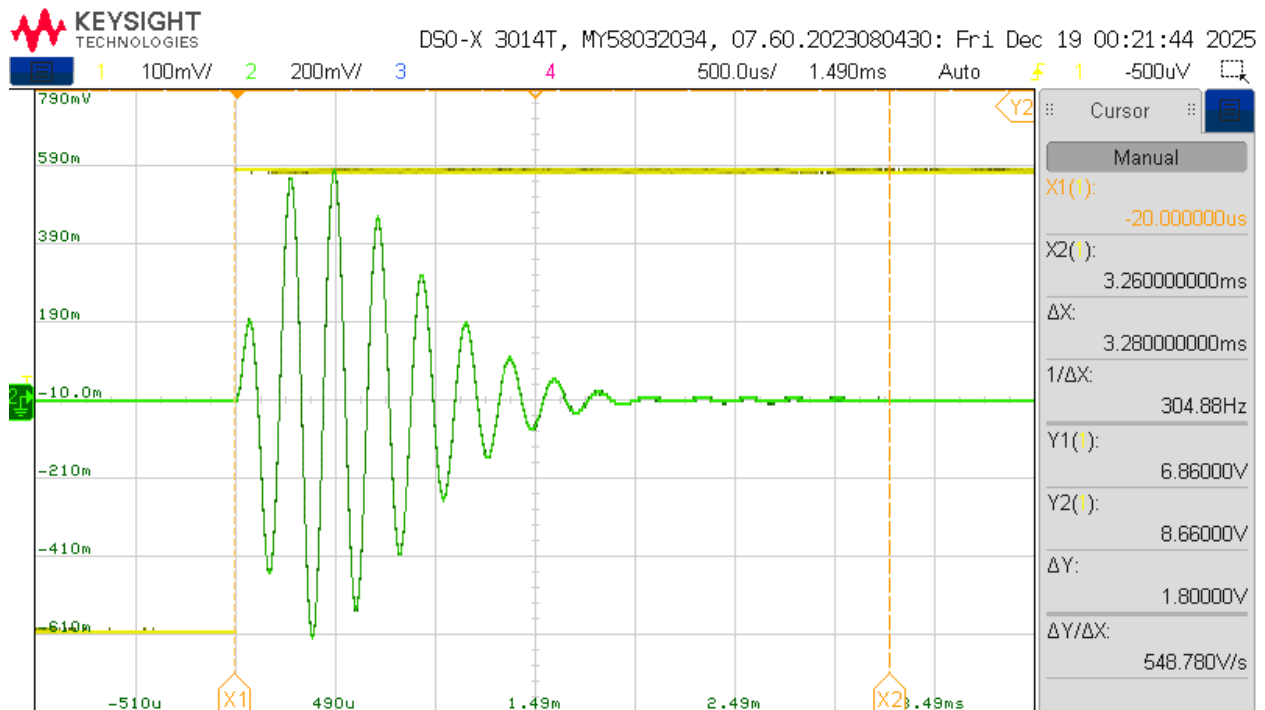


Figure 2.9: Measurement of the filters step response. A 0,5 V square wave was used as the step function.

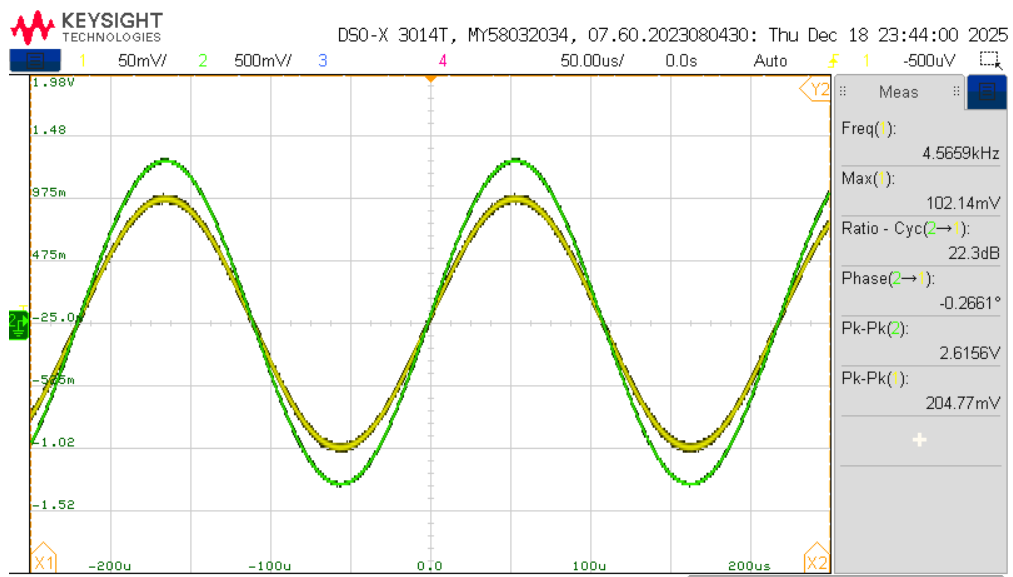


Figure 2.10: Measurement of the passband gain.

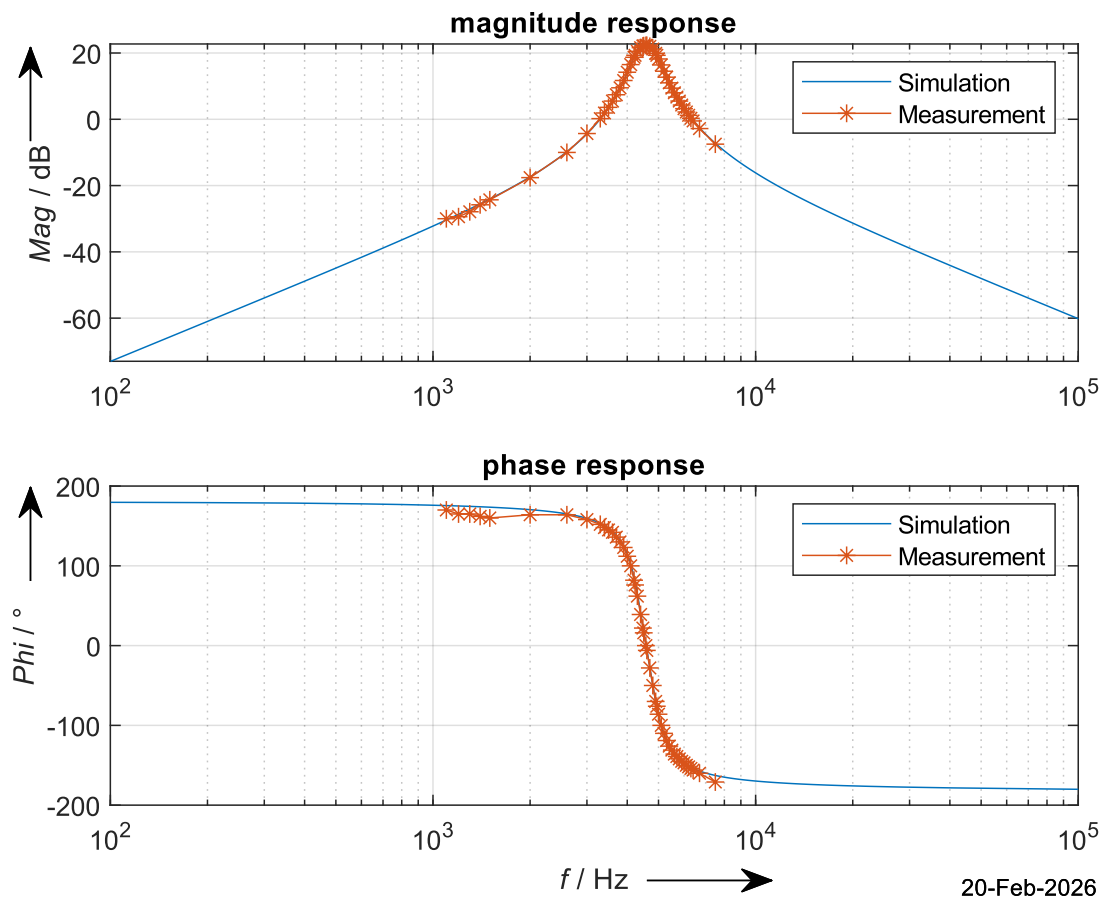


Figure 2.11: Bode plot displaying both simulated and measured values.

2.1.6 Discussion of Measurement Results

2.2 ADC-Driver And Anti-aliasing Filter

2.2.1 Task Description

A single-ended to differential driver for the AD7626 ADC was designed using the LM4562 dual operational amplifier. The circuit includes a second-order active low-pass filter (100 Hz – 40 kHz) with a total differential gain of 20 and a DC offset of 1 V at both outputs.

The circuit was simulated in PSpice (Bode plot, time-domain response and output noise), implemented on a prototype board, and experimentally characterized. Magnitude and phase response, step response, and differential output signals were measured and compared with the simulation results.

Finally, the SNR and ENOB were calculated for a full-scale ADC input signal.

| | |
|----------|--------|
| C_1 | 150 pF |
| C_2 | 4,7 nF |
| f_{cl} | 100 Hz |
| f_{cu} | 40 kHz |
| A_0 | 20 |

Table 2.4: Given values.

2.2.2 Schematic

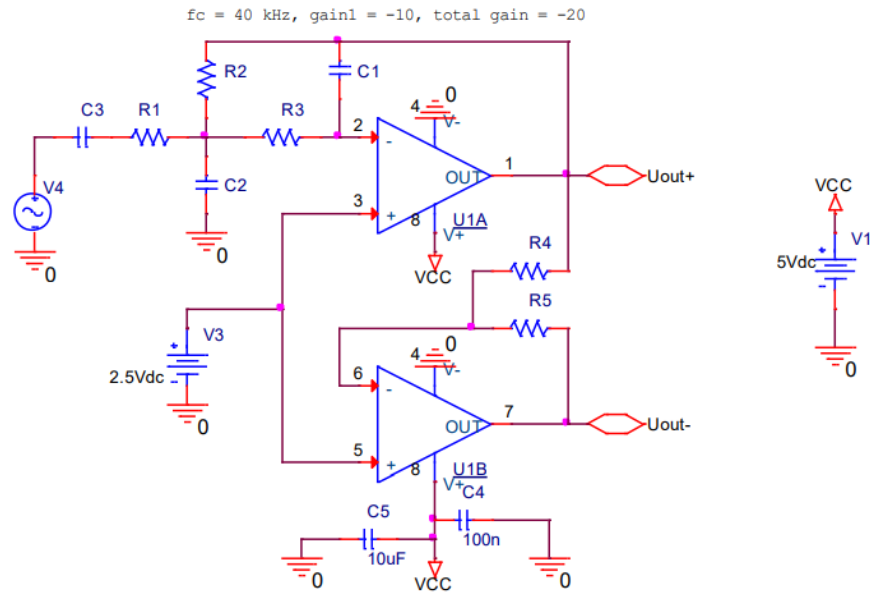


Figure 2.12: Schematic of the ADC driver with anti-aliasing filter

2.2.3 Formulas and Calculations

To calculate the component values the general transfer function for

$$H(s) = \frac{H_0}{1 + a \cdot s + b \cdot s^2} \quad (2.1)$$

$$H(P) = -\frac{\frac{R_2}{R_1}}{1 + \omega_c C_1 \left(R_2 + R_3 + \frac{R_2 R_3}{R_1} \right) P + \omega_c^2 C_1 C_2 R_2 R_3 P^2} \quad (2.2)$$

$$H_0 = -\frac{R_2}{R_1} \quad (2.3)$$

$$a = \omega_c C_1 \left(R_2 + R_3 + \frac{R_2 R_3}{R_1} \right) \quad (2.4)$$

$$b = \omega_c^2 C_1 C_2 R_2 R_3 \quad (2.5)$$

$$P = \frac{s}{\omega_c} \quad (2.6)$$

The decision was made to use a Butterworth characteristic for the second order multi-feedback filter. The values for a and b for a Butterworth filter are as follows:

$$a = \sqrt{2} \quad (2.7)$$

$$b = 1 \quad (2.8)$$

ω_c is calculated according to equation 2.9.

$$\omega_c = 2\pi f_{cu} = 2\pi \cdot 40 \text{ kHz} = 251 \cdot 10^3 \text{ s}^{-1} \quad (2.9)$$

SNR and ENOB Calculation of the ADC Driver System

The system consists of a single-ended to differential driver implemented with the LM4562 operational amplifier, followed by the AD7626 16-bit ADC. The total system performance is limited by both the ADC quantization noise and the analog front-end noise.

Ideal ADC SNR

For an ideal N-bit ADC with a full-scale sinusoidal input, the theoretical Signal-to-Noise Ratio (SNR) is given by:

$$SNR_{ideal} = 6.02N + 1.76 \text{ [dB]} \quad (2.10)$$

For a 16-bit ADC:

$$SNR_{ideal} = 6.02 \cdot 16 + 1.76 = 98.08 \text{ dB} \quad (2.11)$$

This value represents the quantization noise limit only.

Real ADC SNR (Datasheet Value)

According to the AD7626 datasheet, the typical SNR for a full-scale sine wave is:

$$SNR_{ADC} \approx 91.5 \text{ dB} \quad (2.12)$$

This value includes internal non-idealities and thermal noise.

Analog Driver Signal Level

The input signal to the driver is:

$$V_{in,pp} = 100 \text{ mV} \quad (2.13)$$

The differential gain of the driver is:

$$A_{diff} = 20 \quad (2.14)$$

Therefore, the peak-to-peak voltage at the ADC input is:

$$V_{out,pp} = A_{diff} \cdot V_{in,pp} = 20 \cdot 0.1 = 2 \text{ V} \quad (2.15)$$

RMS Signal Value at the ADC Input

For a sinusoidal signal:

$$V_{signal,RMS} = \frac{V_{pp}}{2\sqrt{2}} = \frac{2}{2\sqrt{2}} = \frac{2}{2.828} = 0.707 \text{ V} \quad (2.16)$$

RMS Noise Voltage of the Driver

From PSpice noise simulation over the bandwidth (100 Hz – 40 kHz):

$$V_{noise,RMS} = 40.7 \mu\text{V} \quad (2.17)$$

Driver SNR

$$SNR_{driver} = \frac{V_{signal,RMS}}{V_{noise,RMS}} = \frac{0.707}{40.7 \times 10^{-6}} = 17375 \quad (2.18)$$

In decibels:

$$SNR_{driver,dB} = 20 \log_{10}(17375) = 84.8 dB \quad (2.19)$$

Total System SNR

Since ADC noise and driver noise are uncorrelated, they must be combined in linear scale:

$$\frac{1}{SNR_{total}} = \frac{1}{SNR_{ADC}} + \frac{1}{SNR_{driver}} \quad (2.20)$$

First, convert both SNR values to linear scale:

$$SNR_{ADC,lin} = 10^{91.5/10} = 1.41 \times 10^9 \quad (2.21)$$

$$SNR_{driver,lin} = 10^{84.8/10} = 3.02 \times 10^8 \quad (2.22)$$

Combine both contributions:

$$\frac{1}{SNR_{total,lin}} = \frac{1}{1.41 \times 10^9} + \frac{1}{3.02 \times 10^8} \quad (2.23)$$

$$SNR_{total,lin} \approx 2.48 \times 10^8 \quad (2.24)$$

Convert back to decibels:

$$SNR_{total,dB} = 10 \log_{10}(2.48 \times 10^8) = 83.95 dB \quad (2.25)$$

Effective Number of Bits (System)

$$ENOB = \frac{SNR_{total,dB} - 1.76}{6.02} = \frac{83.95 - 1.76}{6.02} = \frac{82.19}{6.02} = 13.65 bits \quad (2.26)$$

2.2.4 Table(s) with Measurement Results

Table 2.5: Component values for ADC driver and anti-aliasing filter

| | Calculated | Chosen | Measured |
|--------------------|------------|--------|----------|
| R_1 in Ω | - | 820 | 817 |
| R_2 in $k\Omega$ | - | 8.2 | 8.1602 |
| R_3 in $k\Omega$ | - | 2.7 | 2.6888 |
| R_4 in $k\Omega$ | 10 | 10 | 9.8642 |
| R_5 in $k\Omega$ | 10 | 10 | 9.8666 |
| C_1 in pF | - | 150 | 155 |
| C_2 in nF | - | 4.7 | 4.61 |
| C_3 in μF | - | 1.5 | 1.56 |
| C_4 in nF | - | 100 | - |
| C_5 in μF | - | 10 | - |

The measured resistor deviations are within the expected 1% tolerance range. The small deviations of the RC components slightly influence the cutoff frequency of the anti-aliasing filter, but remain within acceptable limits. The measured capacitance variation of C1 (150 pF \rightarrow 155 pF) leads to a minor shift of the pole frequency.

The measurements for the bode plot can be found at the appendix in table A.2

The measured response shows a constant gain of approximately 26 dB within the passband. The phase shift approaches -180 deg at high frequencies, which confirms the expected second-order low-pass behavior. The cutoff frequency can be determined from the -3 dB drop relative to the mid-band gain.

2.2.5 Curves & Diagrams

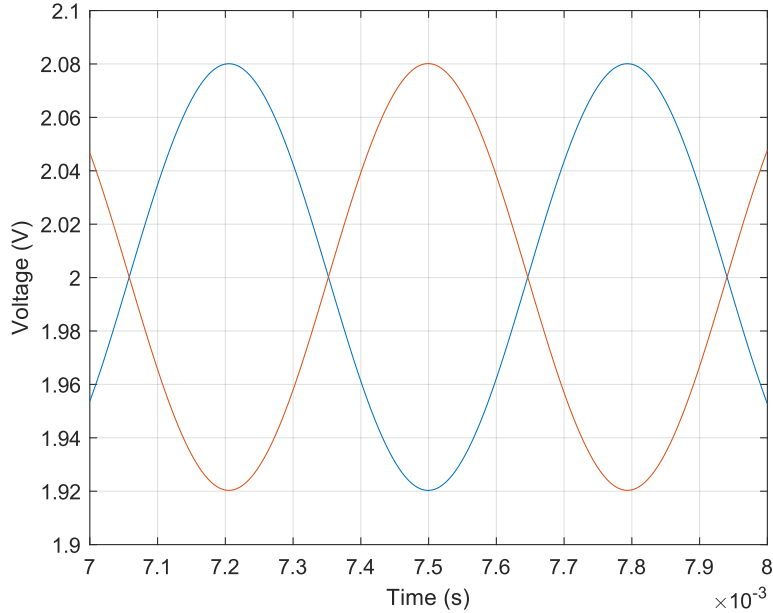


Figure 2.13: Simulation results of the ADC driver and anti-aliasing filter. The blue line shows the non-inverted output, while the orange line shows the inverted output. The offset voltage is 2 V. The input sine wave has an amplitude of 8 mV.

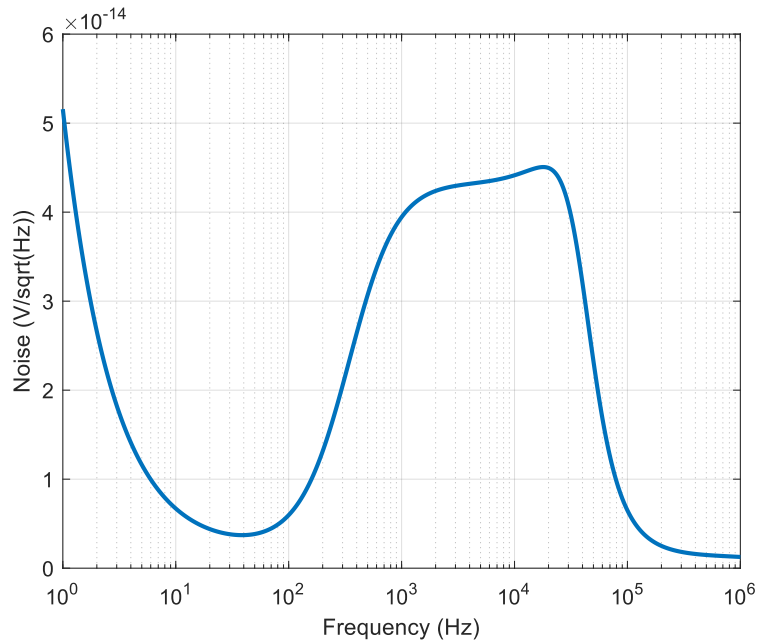


Figure 2.14: Simulation results of the noise spectral voltage density.

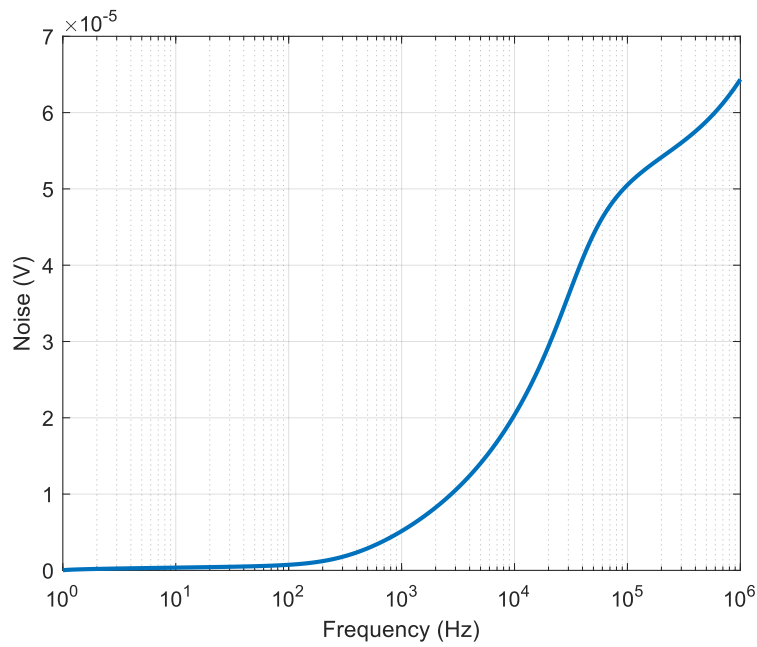


Figure 2.15: Simulation results of the total output noise.

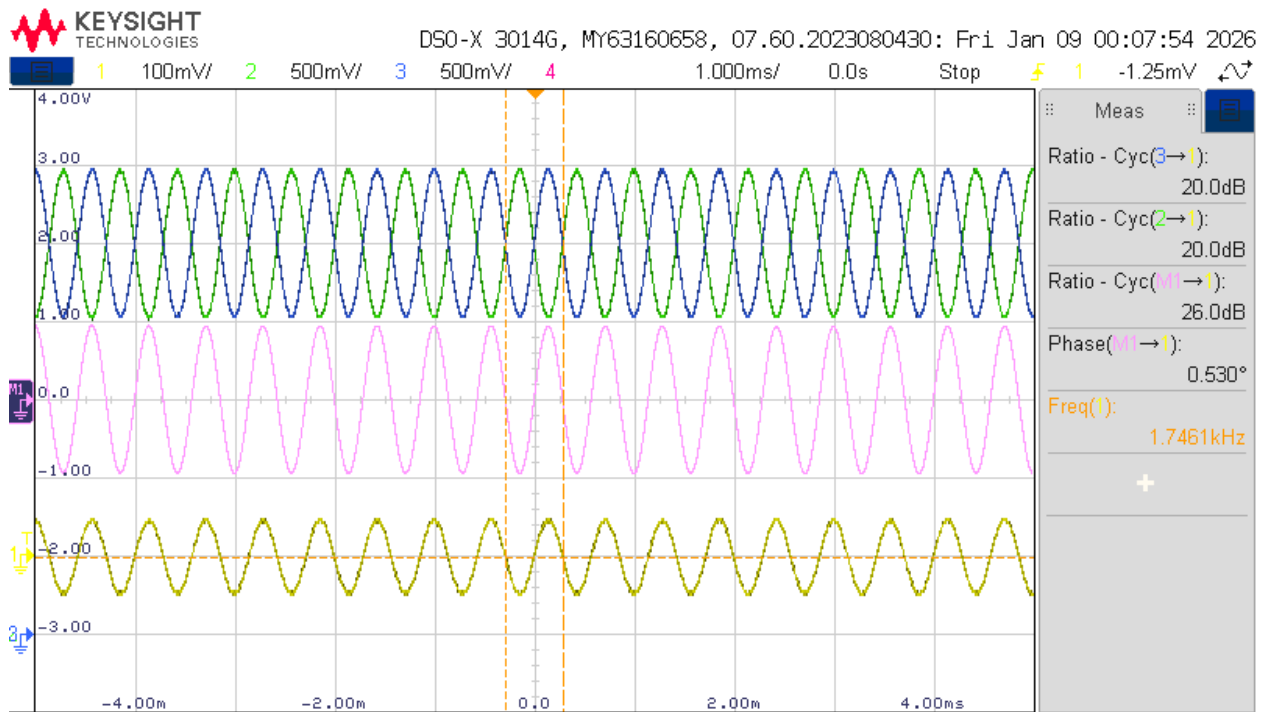


Figure 2.16: Measurements of input signal (yellow), the non-inverting (blue) and inverting (green) output and the differential output (magenta).

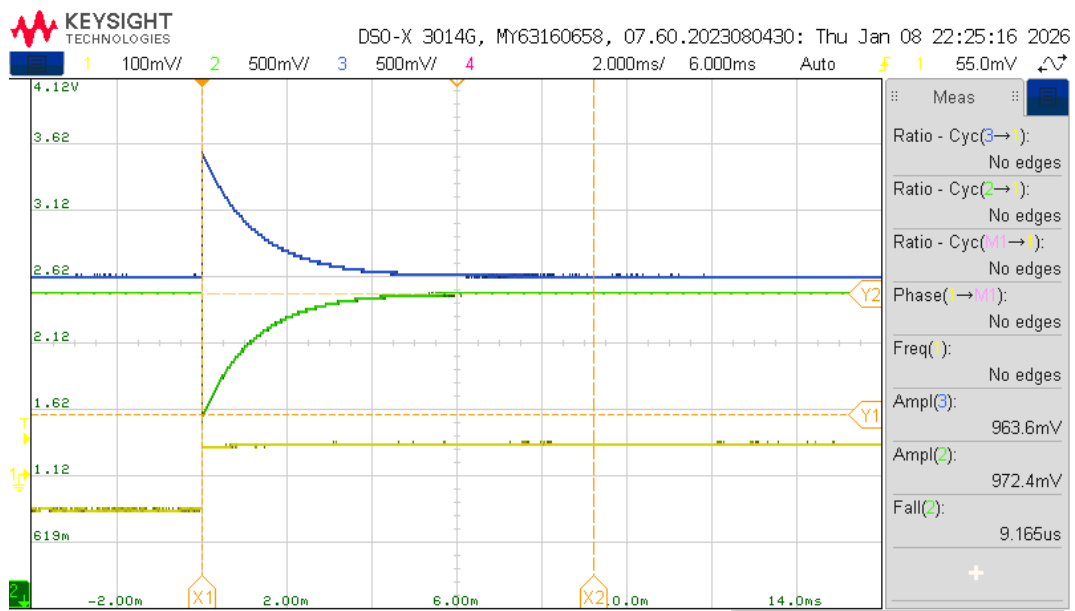


Figure 2.17: Step response of the ADC driver and anti-aliasing filter.

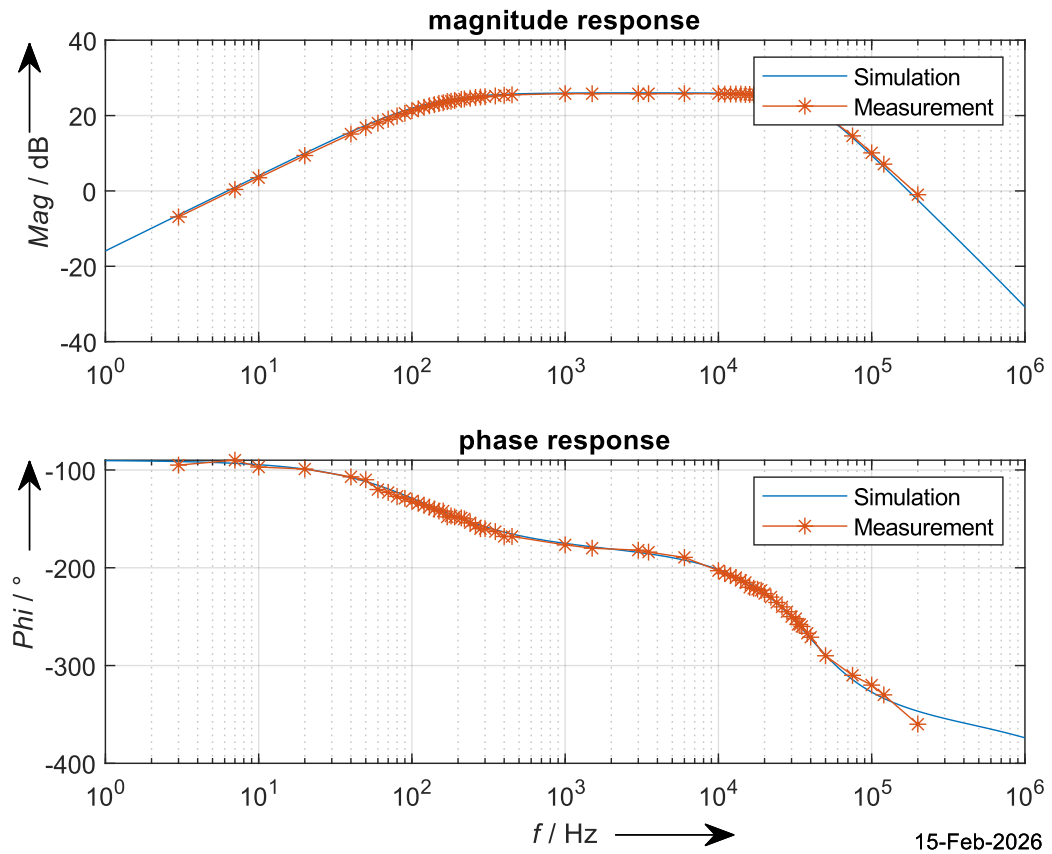


Figure 2.18: Bode plot displaying both simulated and measured values of the differential output.

2.2.6 Discussion of Measurement Results

As we can observe in Figure 2.16, the driver correctly amplifies the input signal, providing a differential gain of approximately 20 (26 dB) in the passband.

The step response (Figure 2.17) shows a typical second-order filter behavior, with an adequate rise time and no significant overshoot.

The comparison between simulation and measurements in the Bode diagram (Figure 2.18) shows good agreement, confirming that the design meets the frequency and gain specifications.

Small deviations in the component values do not significantly affect the system performance, and the anti-aliasing filter fulfills its function of attenuating frequencies above 40 kHz, protecting the ADC from possible aliasing.

Additionally, it is observed that the total noise at the driver output is approximately $40,7 \mu V$ RMS, which contributes to the limitation of the total system SNR.

Obtaining a total SNR of 83.95 dB, the system is capable of achieving an effective resolution of approximately 13.65 bits, which is suitable for many data acquisition applications, although it does not fully exploit the theoretical 16-bit capability of the ADC.

In conclusion, if we wanted to use the full resolution of the ADC, it would be necessary to reduce the driver noise or increase the amplitude of the input signal in order to better utilize the ADC dynamic range.

2.3 Switched Capacitor Filter

2.3.1 Task Description

A 5th-order clock-tunable switched capacitor filter based on the LTC1063 (dual $\pm 5V$ supply) was implemented. A non-inverting preamplifier stage using the LM4562 with a gain of 100 was placed in front of the filter.

The frequency response was measured for two clock frequencies (1 MHz and 500 kHz) and compared in a Bode plot. The filter behavior near the clock frequency was investigated in the time domain, including possible clock feedthrough effects.

The total output noise was measured using additional amplification stages, and the input-referred noise voltage was determined for different source resistances. Finally, the SNR and ENOB were calculated for a full-scale sine wave.

2.3.2 Schematic

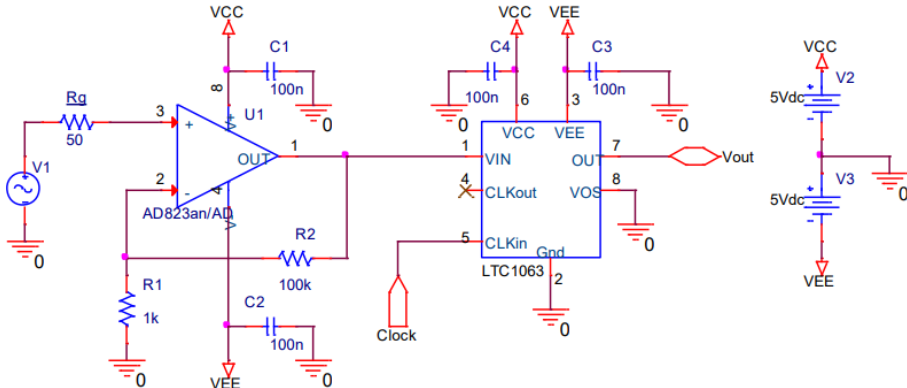


Figure 2.19: Schematic of the switched-capacitor filter with pre-amplifier stage.

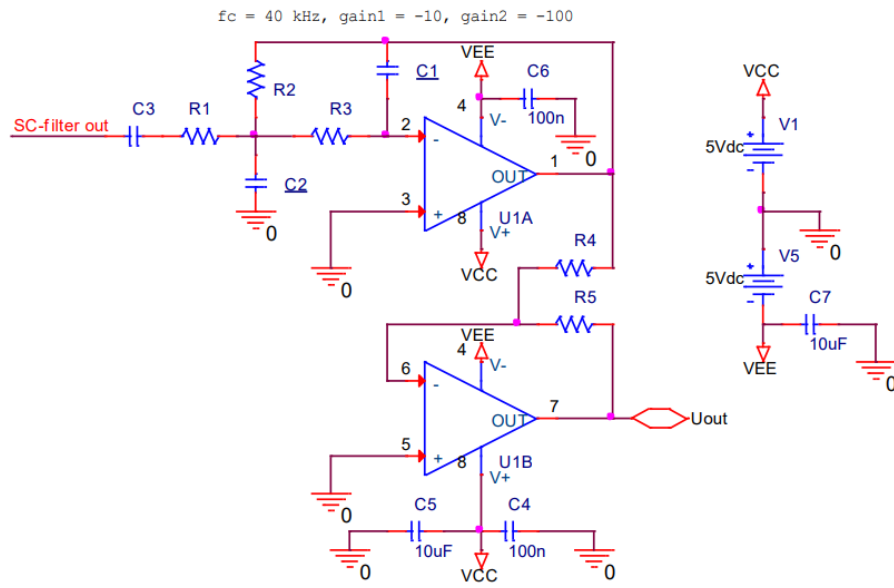


Figure 2.20: Schematic of the low pass filter and amplifier for noise measurement.

2.3.3 Formulas and Calculations

2.3.4 Table(s) with Measurement Results

Table 2.6: Component values for switched capacitor filter

| | Calculated | Chosen | Measured |
|-----------------------|------------|--------|----------|
| R_g in Ω | 50 | 50 | 51.085 |
| R_{g2} in $k\Omega$ | 100 | 100 | 99.959 |
| R_1 in Ω | - | 1000 | 994.81 |
| R_2 in $k\Omega$ | - | 100 | 99.761 |
| C_1 in nF | - | 100 | - |
| C_2 in nF | - | 100 | - |
| C_3 in nF | - | 100 | - |
| C_4 in nF | - | 100 | - |

Table 2.7: Component values for low pass filter and noise measurement amplifier

| | Calculated | Chosen | Measured |
|--------------------|------------|--------|----------|
| R_1 in Ω | - | 820 | 817 |
| R_2 in $k\Omega$ | - | 8.2 | 8.1602 |
| R_3 in $k\Omega$ | - | 2.7 | 2.6888 |
| R_4 in Ω | 1000 | 1000 | 996.6 |
| R_5 in $k\Omega$ | 100 | 100 | 99.585 |
| C_1 in pF | - | 150 | 155 |
| C_2 in nF | - | 4.7 | 4.61 |
| C_3 in μF | - | 1.5 | 1.56 |
| C_4 in nF | - | 100 | - |
| C_5 in μF | - | 10 | - |
| C_6 in nF | - | 100 | - |
| C_7 in μF | - | 10 | - |

The measured resistor values confirm the 1% tolerance specification. Since the switched capacitor filter cutoff frequency is defined by the clock frequency rather than absolute capacitor values, the passive component tolerances have only minor influence on the filter characteristics.

The measurements for the bode plot can be found at the appendix in table A.3 and A.4.

When reducing the clock frequency from 1 MHz to 500 kHz, the cutoff frequency of the switched capacitor filter decreases proportionally. This confirms the theoretical relationship:

$$f_c \propto f_{CLK}$$

The measured data shows approximately half the cutoff frequency compared to the 1 MHz case, which validates the internal switched capacitor principle. Phase wrapping at $\pm 180^\circ$ is again visible due to measurement representation.

2.3.5 Curves & Diagrams

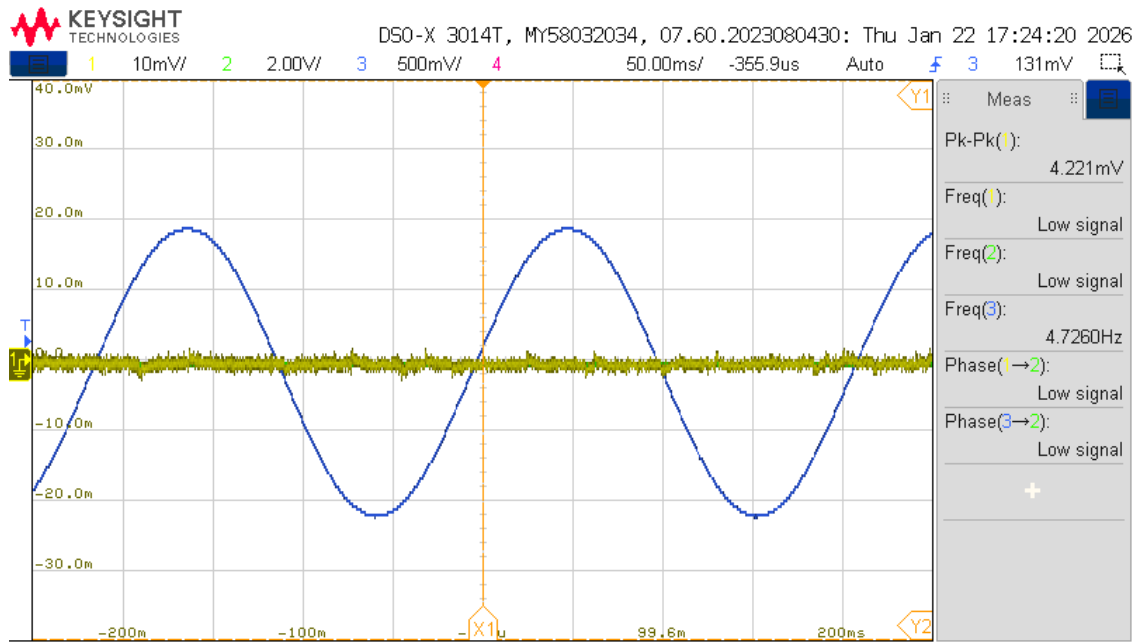


Figure 2.21: Output (blue) of the switched capacitor filter with the input frequency near the tuning frequency.

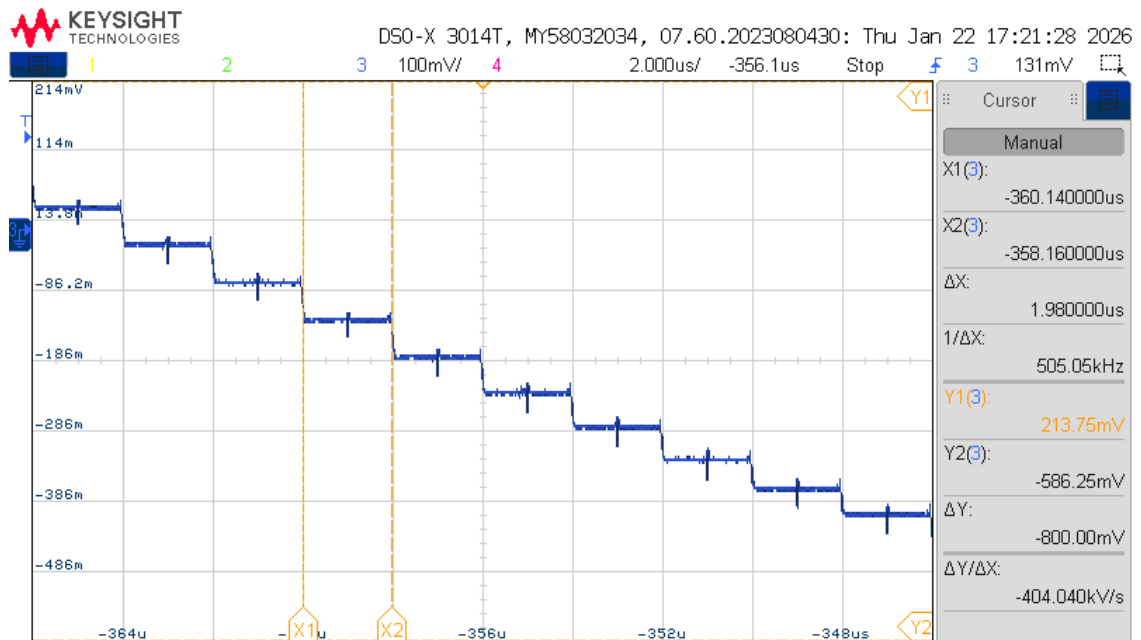


Figure 2.22: Close up of the switched-capacitor filters output signal. Each step is one switching operation of the capacitors.

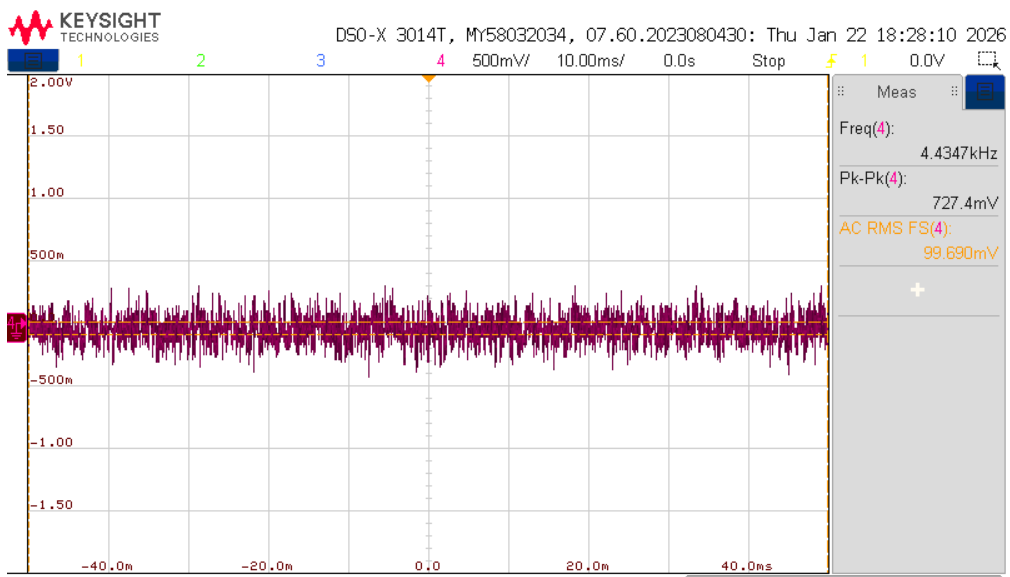


Figure 2.23: Measurement of the total output noise voltage with the input shorted to ground and the SC-filter tuning frequency set to 1 MHz.

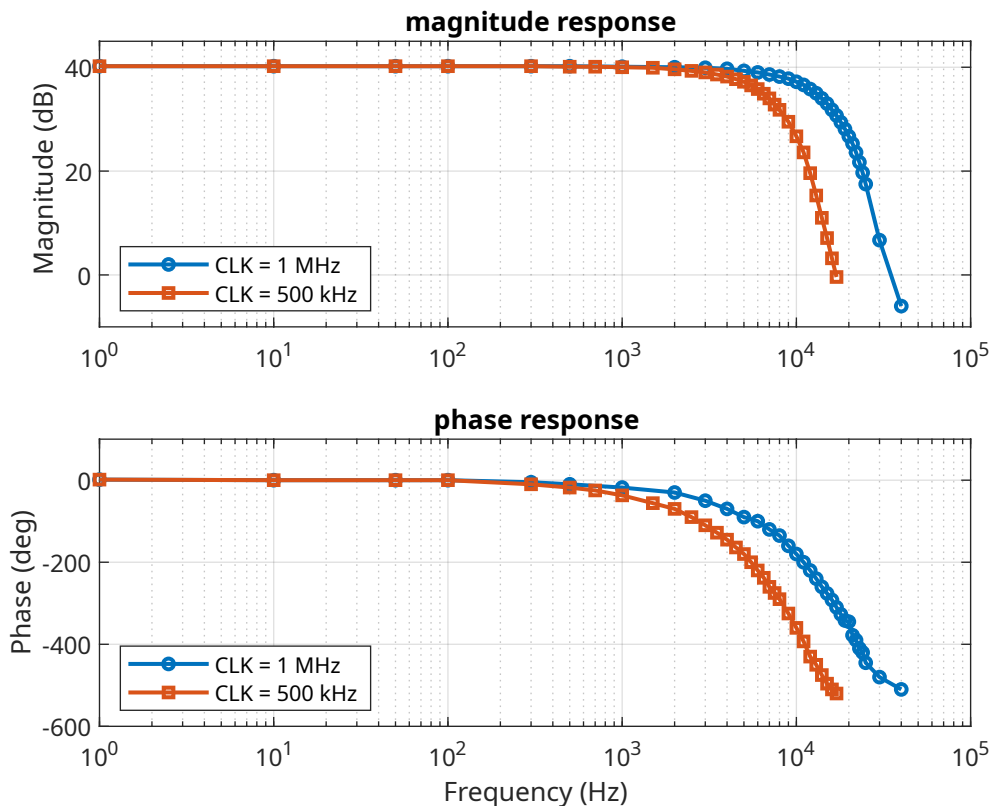


Figure 2.24: Bode plot displaying measured phase and magnitude responses of the switched capacitor filter, one with a tuning frequency of 1 MHz, one with a tuning frequency of 500 kHz.

2.3.6 Discussion of Measurement Results

Equipment

- Benchtop Multimeter

Manufacturer: Agilent
Model: 34450A

- Oscilloscope

Manufacturer: Keysight
Model: DSO-X 3014T

- Function Generator

Manufacturer: Keysight
Model: 33500B

- LCR-Meter

Manufacturer: Keysight
Model: U1733C



Graz, February 20, 2026

Lorenz Buchinger



Agustín Sevil de Llobet

Appendix

A.1 Calculations

A.1.1 Active Band-pass Filter

ACD - Lektur 1

① $U_{C1} + U_{R3} = \emptyset \rightarrow U_{R3} = -U_{C1}$

② $I_1 = \frac{U_{R1}}{R_1} = \frac{U_{in}}{R_1} + \frac{U_{out}}{S C_2 R_2 R_1}$

③ $I_2 = \frac{U_{R2}}{R_2} = -\frac{U_{out}}{S C_2 R_2} \quad U_{C2} = -U_{out} - U_{R2}$

④ $I_{C1} = \frac{U_{C1}}{C_1} = -S(C_1(U_{out} + \frac{U_{out}}{S C_2 R_2}))$

⑤ $U_{C2} + U_{R3} = \emptyset \rightarrow U_{R3} = -U_{C2}$

⑥ $U_{R1} + U_{R3} - U_{in} = \emptyset \rightarrow U_{R1} = U_{in} - U_{R3}$

$I_3 = -\frac{U_{C2}}{R_3} = -\frac{U_{out}}{S C_2 R_2 R_3}$

$I_1 + I_2 = I_3 + I_{C1} \rightarrow \frac{U_{in}}{R_1} + \frac{U_{out}}{S C_2 R_2 R_1} + \frac{U_{out}}{R_2} = -\frac{U_{out}}{S C_2 R_2 R_3} - U_{out} \cdot S C_1 + \frac{U_{out} \cdot C_1}{C_2 R_2}$

$\rightarrow \frac{U_{in}}{R_1} = -U_{out} \left(\frac{1}{R_2} + \frac{C_1}{C_2 R_2} + S C_1 C_2 + \frac{1}{S C_2 R_1 R_2} + \frac{1}{S C_2 R_2 R_3} \right)$

$\rightarrow S \frac{U_{in}}{R_1} = -U_{out} \cdot \left(S \frac{C_1 + C_2}{C_2 R_2} + S^2 C_1 + \frac{R_1 + R_3}{C_2 R_1 R_2 R_3} \right) \rightarrow \frac{U_{out}}{U_{in}} = -\frac{\frac{1}{R_1}}{\frac{R_1 + R_3}{C_2 R_1 R_2 R_3} + S \frac{C_1 + C_2}{C_2 \cdot R_2} + S^2 C_1}$

$\rightarrow H(s) = -\frac{\frac{R_2 \cdot R_3}{R_1 + R_3} \cdot S C_2}{1 + S \frac{R_1 R_3 (C_1 + C_2)}{R_1 + R_3} + S^2 \frac{R_1 R_2 R_3 C_1 C_2}{R_1 R_3}}$

Compare to band Pass \rightarrow 2.5.4 Realisierung Analogschaltung: $P \Rightarrow \frac{1}{\Delta \Omega} (P + \frac{1}{P})$ with $\frac{1}{\Delta \Omega} = Q \Rightarrow S \Rightarrow \frac{S^2 + \omega_0^2}{BS}$

$$H_{LP}(s) = \frac{1}{S^2 + \alpha s + \omega_0^2} \xrightarrow{\text{substitution}} H_{BP}(s) = \frac{1}{(\frac{S^2 + \omega_0^2}{BS})^2 + \alpha \left(\frac{S^2 + \omega_0^2}{BS} \right) + \omega_0^2} \rightarrow B^2 S^2 \rightarrow \omega_0 = 2\pi f_0$$

$$\rightarrow H_{BP}(s) = \frac{B^2 S^2}{(S^2 + \omega_0^2)^2 + \alpha BS(S^2 + \omega_0^2) + \omega_0^2 B^2 S^2} \xrightarrow{33} \begin{cases} (S^2 + \omega_0^2)^2 = S^4 + 2\omega_0^2 S^2 + \omega_0^4 \\ \alpha BS(S^2 + \omega_0^2) = \alpha B S^3 + \alpha B \omega_0^2 S \\ \omega_0^2 B^2 S^2 \end{cases} \rightarrow \text{Polarisation}$$

$$\rightarrow D(s) = S^4 + \alpha B S^3 + (2\omega_0^2 + \omega_0^2 B^2) S^2 + \alpha B \omega_0^2 S + \omega_0^4 \rightarrow \text{Substitute } B \rightarrow$$

$$\rightarrow D_{std}(s) = S^4 + \frac{\omega_0}{Q} S^3 + \left(2\omega_0^2 + \frac{\omega_0^2}{Q^2} \right) S^2 + \frac{\omega_0^3}{Q} S + \omega_0^4$$

Comparison coefficients

$$[1] \quad [2] \quad [3] \quad [4]$$

$$[1] \quad [2] \quad [3] \quad [4]$$

Contract Park & $D_0(s) = s^4 + \frac{\omega_{0i}}{Q} s^3 + \left(2\omega_{0i}^2 + \frac{\omega_{0i}^2}{Q^2}\right) s^2 + \frac{\omega_{0i}^3}{Q} s + \omega_{0i}^4 \rightarrow \omega_{01} = \alpha \omega_0 \quad \omega_{02} = \frac{\omega_0}{\alpha}$

$D_1(s) = s^4 + \frac{\alpha \omega_0}{Q} s^3 + \left(2\alpha^2 \omega_0^2 + \frac{\alpha^2 \omega_0^2}{Q^2}\right) s^2 + \frac{\alpha^3 \omega_0^3}{Q} s + \alpha^4 \omega_0^4$

$D_2(s) = s^4 + \frac{\omega_0}{\alpha Q} s^3 + \left(\frac{2\omega_0^2}{\alpha^2} + \frac{\omega_0^2}{\alpha^2 Q^2}\right) s^2 + \frac{\omega_0^3}{\alpha^3 Q} s + \frac{\omega_0^4}{\alpha^4} \quad D_3(s) = D_1(s) \cdot D_2(s) \rightarrow$

$\rightarrow D_3(s)(s^4 + A_3 s^3 + A_2 s^2 + A_1 s + A_0)(s^4 + B_3 s^3 + B_2 s^2 + B_1 s + B_0)$

$f_L = 4000 \text{ Hz} \quad f_U = 5000 \text{ Hz} \rightarrow f_0 = \sqrt{f_L f_U} = 4472.14 \text{ Hz} \quad \omega_0 = 2\pi \cdot f_0 = 2\pi \cdot 4472.14 = 281098.3$

$BW = f_U - f_L = 1000 \text{ Hz} \quad Q = \frac{f_0}{BW} = 4.42 \quad \Delta \omega_m = \frac{BW}{f_0} = 0.2236 \quad \text{All } C = 10 \mu\text{F}$

Calculation

$P = \frac{1}{\Delta \Omega} \left(P + \frac{1}{P} \right) \text{ with } \frac{1}{\Delta \Omega} = Q \rightarrow H(p) = \frac{H_0}{1 + a_1 \left(\frac{1}{\Delta \Omega} \left(P + \frac{1}{P} \right) \right) + b_1 \left(\frac{1}{\Delta \Omega} \left(P + \frac{1}{P} \right) \right)^2} \rightarrow$

$\rightarrow \frac{H_0}{1 + \frac{a_1 P}{\Delta \Omega} + \frac{a_1}{\Delta \Omega P} + \frac{b_1 P^2}{\Delta \Omega^2} + \frac{2b_1}{\Delta \Omega^2} + \frac{b_1}{\Delta \Omega^2 P^2}} \rightarrow \frac{\frac{\Delta \Omega^2 P^2}{1}}{1} \rightarrow$

$\rightarrow \frac{H_0 \Delta \Omega^2 P^2}{\Delta \Omega^2 P^2 + \frac{a_1 \Delta \Omega^2 P^3}{\Delta \Omega} + \frac{a_1 \Delta \Omega^2 P^2}{\Delta \Omega P} + \frac{b_1 P^4 \Delta \Omega^2}{\Delta \Omega^2} + \frac{2b_1 \Delta \Omega^2 P^2}{\Delta \Omega^2} + \frac{b_1 \Delta \Omega^2 P^2}{\Delta \Omega^2 P^2}} \rightarrow$

$\rightarrow \frac{H_0 \Delta \Omega^2 P^2}{\Delta \Omega^2 P^2 + a_1 \Delta \Omega^2 P^3 + a_1 \Delta \Omega^2 P^2 + b_1 P^4 + 2b_1 P^2 + b_1} \rightarrow \frac{1}{b_1} \rightarrow \frac{\frac{H_0 \Delta \Omega^2 P^2}{b_1}}{\frac{\Delta \Omega^2 P^2}{b_1} + \frac{a_1 \Delta \Omega^2 P^3}{b_1} + \frac{a_1 \Delta \Omega^2 P^2}{b_1} + \frac{b_1 P^4 + 2b_1 P^2 + b_1}{b_1}} \rightarrow$

$\rightarrow \text{Normalization} \rightarrow = \frac{\frac{H_0 \Delta \Omega^2 P^2}{b_1}}{1 + \frac{a_1}{b_1} \Delta \Omega P + \left[2 + \frac{\Delta \Omega^2}{b_1} \right] P^2 + \frac{a_1}{b_1} \Delta \Omega P^3 + P^4}$

Scrib: 1st order Lendyn:

$H(p) = \frac{\frac{H_0}{b_1} \Delta \Omega^2 P^2}{\left[1 + \frac{a_1}{Q_i} P + (\alpha P)^2 \right] \left[1 + \frac{1}{Q_i} \left(\frac{P}{\alpha} \right) + \left(\frac{P}{\alpha} \right)^2 \right]}$

denominator:

$\left[1 + \frac{1}{Q_i} \left(\frac{P}{\alpha} \right) + \left(\frac{P}{\alpha} \right)^2 \right] + \left[\frac{\alpha}{Q_i} P + \frac{\alpha P^2}{Q_i^2 \alpha} + \frac{P^3}{\alpha Q_i} \right] + \left[(\alpha P)^2 + \frac{\alpha P^3}{Q_i} + P^4 \right] \rightarrow P \text{ common denominator} \rightarrow$

$\rightarrow 1 + P \left[\frac{1}{Q_i \alpha} + \frac{\alpha}{Q_i} \right] + P^2 \left[\frac{1}{\alpha^2} + \frac{1}{Q_i^2} + \alpha^2 \right] + P^3 \left[\frac{1}{\alpha Q_i} + \frac{\alpha}{Q_i} \right] + P^4$

2

Escaneado con CamScanner

Figure A.2: Page 2 of the hand written calculations for the active band-pass filter.

Mitfaktor denominieren:

$$1 + P \left[\frac{a_1}{b_1} \Delta \Omega \right] + P^2 \left[2 + \frac{\Delta \Omega^2}{b_1} \right] + P^3 \left[\frac{a_1}{b_1} \Delta \Omega \right] + P^4$$

$$P^1: \frac{1}{Q_i \alpha} + \frac{\alpha}{Q_i} = \frac{a_1}{b_1} \Delta \Omega \rightarrow \frac{1 + \alpha^2}{Q_i \alpha} = \frac{a_1 \Delta \Omega}{b_1} \rightarrow \frac{1}{(1 + \alpha^2)} = \frac{a_1}{b_1 + b_1 \alpha^2} \text{ mit } \Delta \Omega \rightarrow$$

$$\rightarrow \cancel{(1 + \alpha^2)^{-1}} \rightarrow Q_i \alpha = \frac{b_1 + b_1 \alpha^2}{a_1 \Delta \Omega} \rightarrow \frac{1}{\alpha} \rightarrow Q_i = \frac{b_1 + b_1 \alpha^2}{a_1 \Delta \Omega \alpha} \quad \text{I}$$

$$P^2: \frac{1}{\alpha^2} + \frac{1}{Q_i^2} + \alpha^2 = 2 + \frac{\Delta \Omega^2}{b_1} \rightarrow \text{Substitution QI} \rightarrow \frac{1}{\alpha^2} + \frac{1}{\frac{(b_1 + b_1 \alpha^2)^2}{a_1 \Delta \Omega \alpha}} + \alpha^2 = 2 + \frac{\Delta \Omega^2}{b_1}$$

$$\text{Battermann} \quad \left. \begin{array}{l} a_1 = \sqrt{2} \\ b_1 = 1 \end{array} \right\} \text{Tabellen} \quad \Delta \Omega = \frac{f_{max} - f_{min}}{f_0} = \frac{1000}{1472,1} = 0,2236 \quad f_{m1} = \frac{f_0}{\alpha} = 4131,53 \\ f_0 = \sqrt{f_{min} f_{max}} = \sqrt{1400 \cdot 500} = 1472,1 \text{ Hz} \quad f_{m2} = f_0 \alpha = 41840,82$$

$$\text{Solve eq (I) with Tj-mSpire CX II F second} \rightarrow \alpha BW = 1,08244 \rightarrow Q_{BSW} = \frac{b_1 + b_1 \alpha^2}{a_1 \Delta \Omega \alpha} = 634444$$

$$C_1 = C_2 = 10 \text{ nF} \rightarrow C \quad B = \frac{C_1 + C_2}{2 \pi R_2 C_1 C_2} = \frac{2 \times 10}{2 \pi R_2 C^2} = \frac{1}{\pi C R_2} \rightarrow R_2 = \frac{1}{\pi C B} = 488799 \text{ k}\Omega$$

$$H_T = -\frac{C R_2}{2 \pi R_1} = -\frac{R_2}{2 R_1} \rightarrow |H_T| = \frac{R_2}{2 R_1} \Rightarrow R_1 = \frac{R_2}{2 H_T} = 5447,84 \Omega$$

$$H_T = Q_i \Delta \Omega \sqrt{\frac{f_{max}}{b_1}} = 6344 \cdot 0,2236 \cdot \sqrt{\frac{10}{1}} = 4,48618$$

$$R_3 = \frac{R_1}{(R_1 R_2 f_{m1}^2 - 1)(2 \pi C)^2} = 303,59 \Omega$$

BW2:

$$R_S = \frac{1}{\pi C B} \rightarrow B = \frac{f_{m2}}{Q} = 763'005 \rightarrow R_S = 41'7179 \text{ k}\Omega \quad R_4 = \frac{R_S}{2 H_T} = 4649,61 \Omega$$

$$R_6 = \frac{R_4}{(R_4 R_S f_{m2}^2 - 1)(2 \pi C)^2} = 259,107 \Omega$$

Calculated

$$\left. \begin{array}{l} R_1 = 5447,84 \Omega \\ R_2 = 488799 \Omega \\ R_3 = 303,59 \Omega \\ R_4 = 4649,61 \Omega \\ R_S = 41'7179 \Omega \\ R_6 = 259,107 \Omega \end{array} \right\} \text{E24}$$

$$\left. \begin{array}{l} R_1 = 516 \text{ k}\Omega \\ R_2 = 47 \text{ k}\Omega \\ R_3 = 300 \Omega \\ R_4 = 47 \text{ k}\Omega \\ R_S = 43 \text{ k}\Omega \\ R_6 = 270 \Omega \end{array} \right.$$

3

Figure A.3: Page 3 of the hand written calculations for the active band-pass filter.

Chabry 1 Table 12-39, Taitze $\Rightarrow \left\{ \begin{array}{l} a_1 = 1,0650 \\ b_1 = 1,9305 \end{array} \right\}$, solve eq I with $T1-m$ spine CX II- Γ $\Rightarrow Q_i = \frac{\omega_i}{\omega_c} = 1,09712$

$$Q_{m1} = \frac{\omega_0}{\omega_{CH}} = 0,9151,94$$

$$\omega_0 = 4472,13 \quad \Delta\omega = 0,2236 \quad Q_{iCH} = 16,2578$$

$$Q_{m2} = \omega_0 \cdot \omega_{CH} = 4,817,03$$

$$H_F = 16,25 \cdot 0,2236 \cdot \sqrt{\frac{\omega_0}{\omega_1}} = 8,27395 \Rightarrow R_2 = \frac{1}{\pi \cdot B \cdot C} \rightarrow B = \frac{Q_{m1}}{Q_i} = 255,381 \Rightarrow R_2 = 124,641 \text{ k}\Omega$$

$$R_1 = \frac{R_2}{2H_F} = 7,53215 \text{ k}\Omega = R_1$$

$$R_3 = \frac{R_4}{(R_1 R_2 Q_{m1}^2 - 1)(2\pi \cdot C)^2} = 117,89 \Omega$$

$$R_S = \frac{1}{\pi B \cdot C} \rightarrow B = \frac{Q_{m2}}{Q_i} = 296,29 \Rightarrow R_S = 107,432 \text{ k}\Omega$$

$$R_4 = \frac{R_S}{2H_F} = \frac{107,432}{2 \cdot 8,27395} = 6,49219 \text{ k}\Omega = R_4$$

$$R_6 = \frac{R_4}{(R_4 R_S Q_{m2}^2 - 1)(2\pi \cdot C)^2} = 101,613 \Omega$$

calculated €24

| | |
|---------------------------------|-----------------------------|
| $R_1 = 7,53215 \text{ k}\Omega$ | $R_1 = 7,5 \text{ k}\Omega$ |
| $R_2 = 124,641 \text{ k}\Omega$ | $R_2 = 120 \text{ k}\Omega$ |
| $R_3 = 117,89 \Omega$ | $R_3 = 120 \text{ }\Omega$ |
| $R_4 = 6,49219 \text{ k}\Omega$ | $R_4 = 6,2 \text{ k}\Omega$ |
| $R_S = 107,432 \text{ k}\Omega$ | $R_S = 110 \text{ k}\Omega$ |
| $R_6 = 101,613 \Omega$ | $R_6 = 100 \Omega$ |

Escaneado con CamScanner

Figure A.4: Page 4 of the hand written calculations for the active band-pass filter.

A.2 Matlab

A.3 Measurements

Table A.1: Measured frequency response of the active band-pass filter

| Frequency / Hz | Gain / dB | Phase / Degree | Remark |
|----------------|-----------|----------------|--------|
| 1 | -47 | - | |
| 10 | -45 | - | |
| 100 | -45 | - | |
| 1000 | -32 | - | |
| 1100 | -30 | 170 | |
| 1200 | -29.4 | 165 | |
| 1300 | -27.9 | 165 | |
| 1400 | -25.8 | 162 | |

Table A.1: Measured frequency response of the active band-pass filter (continuation)

| Frequency / Hz | Gain / dB | Phase / Degree | Remark |
|----------------|-----------|----------------|---------------------|
| 1500 | -24.3 | 160 | |
| 2000 | -17.6 | 164 | |
| 2600 | -10 | 164 | |
| 3000 | -4.3 | 158 | |
| 3300 | 0.2 | 152 | |
| 3400 | 1.9 | 148 | |
| 3500 | 3.6 | 145 | |
| 3600 | 5.5 | 142 | |
| 3700 | 7.4 | 136 | |
| 3800 | 9.5 | 130 | |
| 3900 | 11.7 | 123 | |
| 4000 | 14.2 | 112 | |
| 4100 | 16.5 | 100 | |
| 4200 | 18.7 | 82 | -3 dB region |
| 4230 | 19.3 | 76 | -3 dB region |
| 4300 | 20.5 | 62 | -3 dB region |
| 4400 | 21.6 | 39 | |
| 4472.13 | 22.1 | 22 | Theoretical f_c |
| 4500 | 22.2 | 16 | |
| 4570 | 22.3 | 0 | Measured f_c |
| 4600 | 22.3 | -6 | |
| 4700 | 22 | -28 | |
| 4800 | 21.2 | -50 | |
| 4900 | 19.9 | -70 | -3 dB region |
| 4940 | 19.3 | -76 | -3 dB region |
| 5000 | 18.2 | -86 | -3 dB region |
| 5100 | 16.4 | -100 | |
| 5200 | 14.5 | -110 | |

Table A.1: Measured frequency response of the active band-pass filter (continuation)

| Frequency / Hz | Gain / dB | Phase / Degree | Remark |
|----------------|-----------|----------------|--------|
| 5300 | 12.7 | -119 | |
| 5400 | 11 | -126 | |
| 5500 | 9.4 | -131 | |
| 5600 | 8 | -136 | |
| 5700 | 6.7 | -139 | |
| 5800 | 5.5 | -142 | |
| 5900 | 4.3 | -145 | |
| 6000 | 3.2 | -147 | |
| 6100 | 2.2 | -150 | |
| 6200 | 1.2 | -152 | |
| 6300 | 0.3 | -154 | |
| 6400 | -0.5 | -156 | |
| 6700 | -2.8 | -160 | |
| 7500 | -7.5 | -171 | |
| 8000 | -9.7 | - | |
| 9000 | -13.3 | - | |
| 10000 | -16.4 | - | |
| 50000 | -32.5 | - | |

Table A.2: Measured frequency response of the ADC-driver and anti-aliasing filter

| Frequency / Hz | Gain / dB | Phase / Degree |
|----------------|-----------|----------------|
| 3 | -6.80 | 80 |
| 7 | 0.40 | 85 |
| 10 | 3.40 | 87 |
| 20 | 9.30 | 80 |
| 40 | 15.00 | 73 |
| 50 | 16.80 | 69 |

Table A.2: Measured frequency response of the ADC-driver and anti-aliasing filter (continuation)

| Frequency / Hz | Gain / dB | Phase / Degree |
|----------------|-----------|----------------|
| 60 | 18.10 | 66 |
| 70 | 19.20 | 61 |
| 80 | 20.10 | 59 |
| 90 | 20.90 | 56 |
| 100 | 21.50 | 54 |
| 110 | 22.00 | 51 |
| 120 | 22.40 | 48 |
| 130 | 22.80 | 46 |
| 135 | 23.00 | 45 |
| 140 | 23.10 | 44 |
| 150 | 23.40 | 42 |
| 160 | 23.70 | 40 |
| 170 | 23.90 | 38 |
| 180 | 24.10 | 36 |
| 190 | 24.20 | 35 |
| 200 | 24.40 | 34 |
| 210 | 24.50 | 33 |
| 220 | 24.60 | 31 |
| 230 | 24.70 | 30 |
| 240 | 24.80 | 29 |
| 260 | 25.00 | 27 |
| 280 | 25.10 | 25 |
| 300 | 25.20 | 24 |
| 330 | 25.40 | 22 |
| 350 | 25.40 | 20 |
| 400 | 25.60 | 18 |
| 450 | 25.70 | 16 |
| 500 | 25.80 | 14 |

Table A.2: Measured frequency response of the ADC-driver and anti-aliasing filter (continuation)

| Frequency / Hz | Gain / dB | Phase / Degree |
|----------------|-----------|----------------|
| 600 | 25.80 | 10 |
| 750 | 25.90 | 8 |
| 825 | 25.90 | 7 |
| 1000 | 26.00 | 6 |
| 1250 | 26.00 | 4 |
| 1500 | 26.00 | 2 |
| 1750 | 26.00 | 0 |
| 2250 | 26.00 | -1 |
| 2500 | 26.00 | -2 |
| 2750 | 26.00 | -3 |
| 3000 | 26.00 | -4 |
| 3500 | 26.00 | -5 |
| 6000 | 26.00 | -11 |
| 10000 | 25.90 | -18 |
| 11000 | 25.90 | -21 |
| 12000 | 25.90 | -23 |
| 13000 | 25.80 | -28 |
| 14000 | 25.80 | -30 |
| 15000 | 25.80 | -31 |
| 16000 | 25.70 | -34 |
| 17000 | 25.70 | -35 |
| 18000 | 25.60 | -37 |
| 19000 | 25.60 | -40 |
| 20000 | 25.50 | -42 |
| 22000 | 25.40 | -48 |
| 24000 | 25.20 | -54 |
| 26000 | 25.00 | -56 |
| 28000 | 24.70 | -60 |

Table A.2: Measured frequency response of the ADC-driver and anti-aliasing filter (continuation)

| Frequency / Hz | Gain / dB | Phase / Degree |
|----------------|-----------|----------------|
| 30000 | 24.40 | -66 |
| 32000 | 24.10 | -72 |
| 33000 | 24.00 | -75 |
| 34000 | 23.80 | -75 |
| 35000 | 23.60 | -78 |
| 37000 | 23.20 | -80 |
| 38000 | 23.00 | -83 |
| 39000 | 22.80 | -84 |
| 40000 | 22.60 | -86 |
| 45000 | 21.50 | -93 |
| 50000 | 20.40 | -106 |
| 55000 | 19.20 | -109 |
| 60000 | 18.00 | -114 |
| 65000 | 16.90 | -120 |
| 70000 | 15.50 | -122 |
| 75000 | 14.50 | -125 |
| 100000 | 9.90 | -130 |
| 120000 | 6.80 | -140 |
| 150000 | 3.30 | -156 |
| 190000 | 0.00 | -180 |
| 200000 | -1.00 | -180 |

Table A.3: Measured frequency and phase response of switched capacitor filter with a tuning frequency of 500 kHz

| Input Frequency / Hz | Gain / dB | Phase / Degree |
|----------------------|-----------|----------------|
| 1 | 40.2 | 1.4 |
| 10 | 40.2 | 0 |
| 50 | 40.2 | 0 |

Table A.3: Measured frequency and phase response of switched capacitor filter with a tuning frequency of 500 kHz (continuation)

| Input Frequency / Hz | Gain / dB | Phase / Degree |
|-----------------------------|------------------|-----------------------|
| 100 | 40.2 | 0 |
| 300 | 40.2 | -10 |
| 500 | 40.1 | -18 |
| 700 | 40.1 | -25 |
| 1000 | 40.0 | -37 |
| 1500 | 39.9 | -56 |
| 2000 | 39.6 | -70 |
| 2500 | 39.3 | -90 |
| 3000 | 39.0 | -110 |
| 3500 | 38.6 | -128 |
| 4000 | 38.2 | -145 |
| 4500 | 37.7 | -164 |
| 5000 | 37.2 | 180 |
| 5500 | 36.5 | 160 |
| 6000 | 35.8 | 140 |
| 6500 | 34.9 | 122 |
| 7000 | 34.0 | 100 |
| 7500 | 32.8 | 85 |
| 8000 | 31.8 | 70 |
| 9000 | 29.5 | 35 |
| 10000 | 26.7 | 0 |
| 11000 | 23.6 | -33 |
| 12000 | 19.6 | -70 |
| 13000 | 15.3 | -90 |
| 14000 | 11.0 | -115 |
| 15000 | 7.1 | -136 |
| 16000 | 3.2 | -150 |

Table A.3: Measured frequency and phase response of switched capacitor filter with a tuning frequency of 500 kHz (continuation)

| Input Frequency / Hz | Gain / dB | Phase / Degree |
|-----------------------------|------------------|-----------------------|
| 17000 | -0.4 | -160 |

Table A.4: Measured frequency and phase response of switched capacitor filter with a tuning frequency of 1 MHz

| Input Frequency / Hz | Gain / dB | Phase / Degree |
|-----------------------------|------------------|-----------------------|
| 1 | 40.2 | 1.33 |
| 10 | 40.2 | 0 |
| 50 | 40.2 | 0 |
| 100 | 40.2 | 0 |
| 300 | 40.2 | -5 |
| 500 | 40.2 | -10 |
| 1000 | 40.1 | -18 |
| 2000 | 40.0 | -30 |
| 3000 | 39.9 | -50 |
| 4000 | 39.7 | -70 |
| 5000 | 39.3 | -90 |
| 6000 | 39.0 | -100 |
| 7000 | 38.6 | -120 |
| 8000 | 38.2 | -135 |
| 9000 | 37.8 | -160 |
| 10000 | 37.2 | 180 |
| 11000 | 36.6 | 160 |
| 12000 | 35.8 | 140 |
| 13000 | 35.0 | 120 |
| 14000 | 34.0 | 100 |
| 15000 | 33.0 | 84 |
| 16000 | 31.8 | 68 |

Table A.4: Measured frequency and phase response of switched capacitor filter with a tuning frequency of 1 MHz (continuation)

| Input Frequency / Hz | Gain / dB | Phase / Degree |
|-----------------------------|------------------|-----------------------|
| 17000 | 30.7 | 50 |
| 18000 | 29.4 | 33 |
| 19000 | 28.1 | 18 |
| 20000 | 26.7 | 15 |
| 21000 | 25.3 | -18 |
| 22000 | 23.6 | -30 |
| 23000 | 21.7 | -50 |
| 24000 | 19.7 | -60 |
| 25000 | 17.5 | -85 |
| 30000 | 6.7 | -120 |
| 40000 | -6.0 | -150 |